

Sustainable road alignment planning in the built environment based on the MCDM-GIS method

Feng Jiang^a, Ling Ma^{a,*}, Tim Broyd^a, Ke Chen^b, Hanbin Luo^b, Yang Pei^a

^a The Bartlett School of Sustainable Construction, University College London, 1-19 Torrington Place, London WC1E 6BT, UK

^b School of Civil and Hydraulic Engineering, Huazhong University of Science and Technology, Wuhan 430074, China



ARTICLE INFO

Keywords:

Urban road planning
Building demolition
Noise
Air pollution
MCDM
GIS

ABSTRACT

Sustainable road planning in the cities' built-up areas strives to meet traffic demands of society within limited spaces available for construction and various constraints in the built environment considering engineering, traffic, economic, social, and environmental factors. Unlike rural areas, road planning in the built environment can be significantly influenced by the surroundings, such as existing buildings, road network, and land use, and should consider noise and air pollution impact on residents. In addition, road width and road widening are significant factors for road alignment planning. Based on the MCDM-GIS method, the least-cost wide path algorithm is employed for sustainable road alignment planning in the built environment, considering building demolition and land use, traffic congestion, noise impact, air pollution impact, and construction costs. Road width, new road construction, and existing road widening are considered simultaneously. Several methods are proposed to digitalise and parse various sustainable factors into understandable expressions for road alignment planning. Forbidden areas and road buffer areas for road widening are defined. The proposed method is implemented in road planning in Dartford, Kent County, UK. Sustainable factors with different weights can generate various road alignments from different perspectives, and road widths can significantly and locally influence road alignments.

1. Introduction

In addition to reasonable traffic planning, road planning and construction is always regarded as one of the most fundamental ways to solve traffic congestion in the city's built-up area. Decision-makers and planners are committed to providing sustainable road planning to cope with current and future traffic-related demands and achieve financial, environmental, and social goals without compromising the ability of future generations to meet any needs of their own (Addanki & Venkataraman, 2017). However, fewer spaces are available for road construction in cities' built-up areas (Karki & Lu, 2015). It is challenging for road planning in a city to become sustainable, and traffic congestion always exists. Unlike road planning in the natural environment in rural areas, road planning in cities is conducted in the built environment. Thus, it is inevitably affected by the limited remaining space, existing road networks, existing buildings, land use, traffic congestion, and other factors (Bindajam & Mallick, 2020; Lazda & Smirnovs, 2011). In addition, noise and air pollution impact on residents should be considered (Dobrilović et al., 2022; El Fazziki et al., 2017). Therefore, the alignment

of a road in cities' built-up areas cannot be planned as flexibly as that of a road in rural areas. In addition, existing road widening as well as new road construction should be considered simultaneously to alleviate traffic congestion in the limited urban space (Muneera & Karuppanagounder, 2022). Road alignment planning in the built environment is a complex and interdisciplinary issue that needs to consider many factors, which can be categorised into demands and constraints. On the one hand, road planning in the built environment aims to meet the functional demands of society, especially traffic-related demands (Zeng et al., 2021). On the other hand, road planning in the built environment needs to consider the constraints brought by the limited remaining space, engineering factors, economic considerations, social requirements, and environmental requirements (Gössling, 2020). From the perspective of functional considerations, road planning in the built environment should strive to alleviate traffic congestion by leveraging limited space and existing road networks (Zhong & Liu, 2021). From the perspective of economic considerations, road planning in the built environment needs to reduce building demolition costs, land use costs and construction costs as much as possible, under the premise of

* Corresponding author.

E-mail address: l.ma@ucl.ac.uk (L. Ma).

satisfying traffic-related functions (Mondal et al., 2021). In addition, road planning schemes should facilitate the development of the regional economy (Davis & Jha, 2011). From the perspective of people-friendly, road planning in the built environment should minimise the impacts of demolition, air pollution, and noise on city dwellers to provide a relatively healthy and comfortable living environment (Khomenco et al., 2020). From the perspective of eco-friendly, road planning in the built environment should cause as little negative impact on the environment as possible, such as air, soil, water and noise pollution, and the occupation of green space and vegetation (Font et al., 2014; Garcia-Chan et al., 2021).

Road alignment planning methods can be divided into two categories. In the first category, road alignment shapes composed of standard alignment elements according to the design specifications, such as straight lines, transition curves, and circular curves, are considered. Then, a parametrically controllable alignment is developed to automatically generate suitable alignments considering various traffic, engineering, economic, social, and environmental factors (Garcia-Chan et al., 2021; Vázquez-Méndez et al., 2021). Some heuristic algorithms are usually employed (Angulo et al., 2012; Vazquez-Mendez et al., 2018; Zhang et al., 2020). In the second category, MCDM-GIS methods are widely used. MCDM (multi-criteria decision making) is employed to analyse and give weights to various factors, and GIS (geographic information system) provides an integrated environment using multiple factors to generate road alignments using the least-cost path algorithms (Aguiar et al., 2021; Pushak et al., 2016; Singh & Singh, 2017). Cost rasters consisting of cells are employed to digitalise various factors in the city. The smaller the cells that make up the cost raster, the more precisely the cost raster can represent the city considering various factors (Sitzia et al., 2014). The selected and consecutively connected cells represent the generated road alignment. Compared with the first category, methods in the second category ignore the standard alignment elements. However, in the built environment, the shape of a road alignment is constrained by as-is buildings, road networks, and land use. Thus, in some areas, the shape of the alignment of the planned road can be forced to form (Scoppa et al., 2018). The methods in the second category are more flexible in generating horizontal road alignment than the methods in the first category. In addition, MCDM-GIS methods can easily be employed to parse, analyse, and evaluate various factors comprehensively, and an optimum and sustainable road alignment can be generated automatically on the cost raster. For sustainable road alignment planning in cities based on MCDM-GIS methods, in addition to MCDM analysis and least-cost path analysis, how to collect, digitalise and parse various data from the city should be focused on (Jiang et al., 2022). Considering collecting, digitalising, and parsing various factors, Jiang et al., and Luo (2022) proposed DT (digital twin)-MCDM-GIS framework for sustainable urban road planning considering building demolition, land use, traffic congestion, driving route selection habits, noise, and air pollutants.

For sustainable road planning in the built environment, the relationship between road width and the surroundings can significantly influence road plans. Most road alignment planning based on the MCDM-GIS method ignores road width. However, road alignment planning in the built environment can be significantly influenced by the high-density surroundings (buildings, road networks, etc.) and should consider noise and air pollution impact on residents compared with road alignment planning in rural areas, as mentioned above. If the large cell size of the cost raster is used to represent road width, the cost raster composed of large cells cannot precisely digitalise and describe the surroundings and various sustainable factors in a city. In addition, most existing studies only consider new road construction and neglect existing road widening. Thus, this paper proposes a systematic method to realise sustainable road alignment planning in the built environment considering road width, existing road widening and new road construction simultaneously in the built environment based on the MCDM-GIS method by refining the least-cost wide path algorithm rather than

the least-cost path (Shirabe, 2016). Then, a cost raster consisting of cells with a small size can describe a precise digital city considering various sustainable factors. Simultaneously, the connection of many cells can represent the width of the road. Traffic congestion, noise, air pollutants, building demolition, land use, and construction cost are considered, and corresponding digitalisation and analysis methods for these factors are proposed.

2. Method

The overall workflow of the method can be described in Fig. 1. First, multi-source data are collected, parsed and digitalised using different methods, such as digital twin, digital image processing, etc., to express various factors, including building demolition and land use, traffic congestion, noise impact, air pollution impact, and construction costs. After that, MCDM methods are employed to evaluate and give weights to various factors to establish cost rasters in the GIS environment. Then, the least-cost path algorithm is updated to the least-cost wide path algorithm to generate the optimal road alignment in the built environment considering road width, new road construction, and existing road widening.

2.1. Building digital twin, demolition and land use

The digital surface model (DSM) and digital terrain model (DTM) can be obtained by field survey (traditional methods, airborne Lidar, etc.) or existing map database. Then the digital difference model (DDM) can be obtained by the differences in elevation between DSM and DTM at each point (① in Fig. 2). The 2D polygons representing buildings (elevations are zero) can be obtained from the vector maps (②, ③, and ④ in Fig. 2). After that, the elevations from DDM in each building's 2D polygon area can be obtained, and the average value of these elevations of each building can be calculated, which is called the building's average height (⑤ in Fig. 2). The buildings' digital twins can be obtained by extruding the building's 2D polygon by the average height along the z-axis (⑥ in Fig. 2). Then, the total areas of a building, considering all the floors, can be estimated by Eqs. (1), where H is the calculated average height of the building, a is the area of the building's 2D polygon, and h is the typical floor to floor height in a building. In the UK h is 3.2m (Old Oak and Park Royal Development Corporation, 2018). It is roughly assumed that the building will not be demolished if its total area A is larger than a threshold T_1 , because its demolition costs may be very high (⑦ in Fig. 2). They are set as forbidden areas (⑧ in Fig. 2). For the buildings that may be demolished, the demolition costs per square metre can be estimated by Eqs. (2), where p is the average property price in the target area, and μ is the amplification coefficient considering the compensation for loss of home and relocation of property owners. Though for a specific building, the demolition costs should be determined by the field survey and negotiation with the property's owner, demolition costs of many buildings in a region can be preliminarily estimated by Eqs. (2) in general from a macro perspective. A building is usually demolished completely if the planned road touches the building. It is assumed that the building occupies n cells on a cost raster. The building should be demolished when the planned road occupies any cell belonging to a building. Thus, the number of cells of a building occupied by the planned road varies from 1 to n . Therefore, the average number of the occupied cells can be calculated by $(1+n)/2$. Thus, the ratio of the actual number of demolished cells to the number of occupied cells is $n/((1+n)/2)$. When n is much larger than 1, the ratio is regarded as 2. That is the reason why there is another coefficient "2" in Eqs. (2). Afterwards, the building's 2D polygons are moved by $C_{demolition}$ along the z-axis. The points on the moved building's 2D polygons (including edges and interiors) are extracted (⑨ in Fig. 2). The outlines of each individual building or each group of connected buildings are extracted, excluding common lines between two connected buildings. Then, the outlines are offset outwards by a small value to limit the points of the building, not to

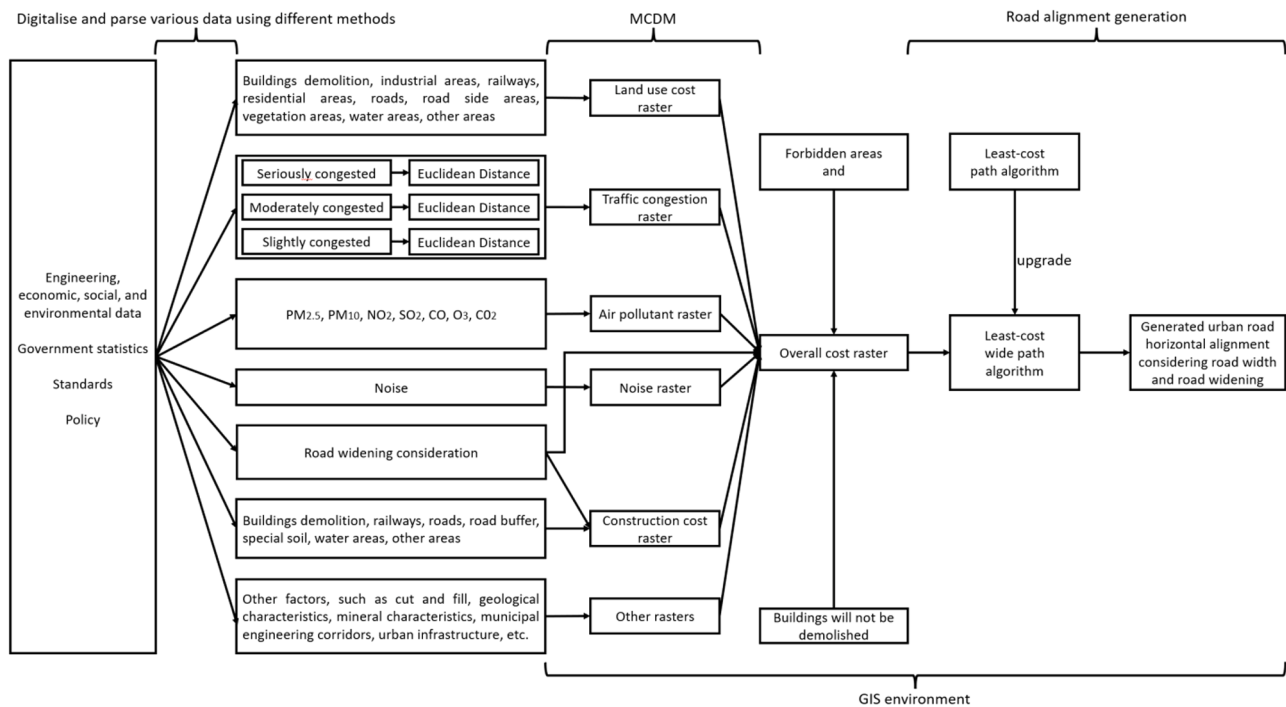


Fig. 1. Overall workflow of road alignment planning in the built environment.

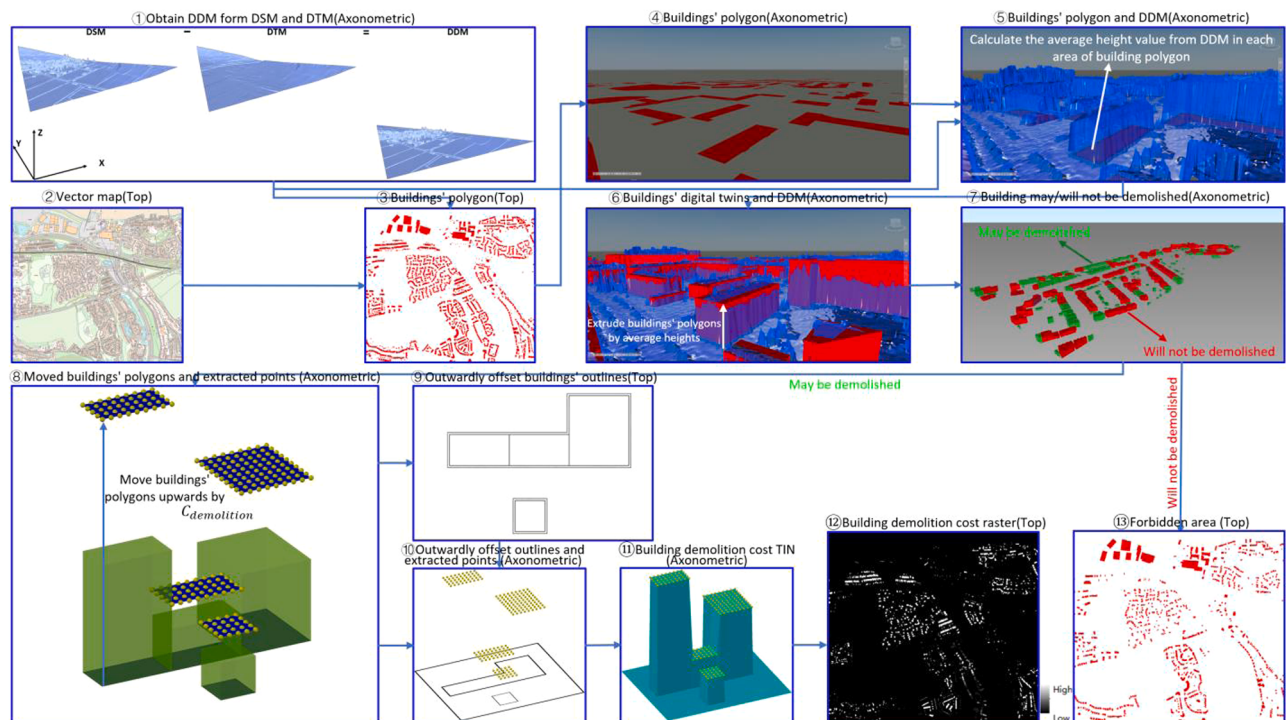


Fig. 2. Building digital twin and demolition costs estimation.

establish the triangles with other building groups in a TIN (Triangulated irregular network) (⑨ in Fig. 2) (Fowler & Little, 1979). After that, the extracted points on the moved building's 2D polygons, the offset outlines of buildings, and the edge of the target area can be put together (⑩ in Fig. 2), and a TIN can be established using them (⑪ in Fig. 2). Then, the TIN can be converted into a raster called building demolition cost raster, and the elevations on the TIN represent the demolition cost (⑫ in Fig. 2).

$$A = \frac{H}{h} a \quad (1)$$

$$C_{demolition} = \frac{2\mu Ap}{a} = \frac{2\mu Hp}{h} \quad (2)$$

The vectors and land values of different types of land, such as agricultural areas, industrial areas, railways, residential areas, roads, roadsides, vegetation areas, water areas, and other areas, can be obtained

from government statistics, as shown in ④ in Fig. 3. Then, the land use cost raster can be established, and its cells' values are the land values (⑤ in Fig. 3). In the areas of the buildings that may be demolished, the values are replaced by the building demolition cost raster (② in Fig. 3). In the areas of the buildings that will not be demolished, the areas on the land use cost raster are set as forbidden areas (③ in Fig. 3). Road alignment planning should avoid occupying the railway area; however, the planned road can cross the railway by tunnels and bridges. Thus, the value of railway areas should be set to the maximin value rather than forbidden areas. Then, the planned road can go across the railway and try to occupy the railways' cells as less as possible on the raster. After that, the land use cost raster should be normalised using fuzzy logic, as shown in ⑥ in Fig. 3 and Eqs. (3), where T_2 is the threshold.

$$Cell_{normalised}(i,j) = \begin{cases} \frac{Cell(i,j)}{T_2}, & cell(i,j) \leq T_2 \\ 1, & cell(i,j) > T_2 \end{cases} \quad (3)$$

2.2. Traffic consideration

Typical traffic congestion situations in the target area can be obtained from Google Maps by screenshots, which are the overall traffic congestion estimates at different times from Monday to Sunday, according to the statistics shown in ① and ② in Fig. 4. R, G, and B should be converted into r, g, and b values for calculation which are rational numbers ranging from 0 to 1. The relationships between R, G, B and r, g, b are shown in Eq. (4). Since the colours representing the traffic congestion situations are typical colours: green, orange, red and dark red, all the colours range from green to red. Thus, these colours can be controlled by the (R-B)/(G-B) values, and their B values are relatively low. Thus, four conditions can extract the colours:

- 1) $(g(i,j)-b(i,j))/(r(i,j)-b(i,j))$ determines if the colour is greener or redder.
- 2) $b(i,j) \leq t_4$: The b value of the colour is very small.
- 3) If the colour is dark red or red, its r value is obviously larger than other values. Thus, $r(i,j) > b(i,j)$. If the colour is orange or yellow, its r

and g values are obviously larger than the b value. Thus, $r(i,j) > b(i,j)$ and $g(i,j) > b(i,j)$. If the colour is green, its g value is obviously larger than other values. Thus, $g(i,j) > b(i,j)$.

- 4) When the colour is red or dark red, $r(i,j)$ determines whether the colour is red or dark red.

The colour extraction process is performed according to Table 1. In the conditions above and Table 1, the $r(i,j)$, $g(i,j)$, and $b(i,j)$ represent the colour values of the (i, j) pixel on the screenshots; $r_e(i,j)$, $g_e(i,j)$, and $b_e(i,j)$ represent the colour values of (i, j) pixel on the new image after extraction (extracted screenshot); t_1 , t_2 , t_3 , t_4 , and t_5 denote the parameters controlling the conditions; the abs denotes the absolute value. The i and j represent the row and column of a pixel on an image, respectively. The images after colour extraction are shown in ③ and ④ in Fig. 4.

$$r = \frac{R}{255}, \quad g = \frac{G}{255}, \quad b = \frac{B}{255} \quad (4)$$

Afterwards, all the extracted screenshots at different times will be fused into an image called the fused traffic image by the RGB colour model, as shown in ⑤ in Fig. 4. The r, g, and b values of the fused traffic images can be calculated using Eqs. (5), where $r_{f,k}(i,j)$, $g_{f,k}(i,j)$, $b_{f,k}(i,j)$ values represent the r, g, and b values of all the extracted screenshots, and k denotes extracted screenshots at different times. The colours on the fused traffic image representing traffic congestion continuously range from green to dark red. Thus, the fused traffic image should be standardised into standard green, orange, yellow, red, and black, as shown in Image ⑥ in Fig. 4. Dark red and red areas are all changed to red. The standardisation process is described in Table 2, where $r_s(i,j)$, $g_s(i,j)$, and $b_s(i,j)$ are the colour values of the standardised traffic image, and t_6 , t_7 , t_8 , t_9 , and t_{10} denote the parameters controlling the conditions. In addition to the four conditions in Table 1, $(r_{fused}(i,j)+g_{fused}(i,j)+b_{fused}(i,j)) > t_{10}$ is used to remove dark areas in the fused traffic image.

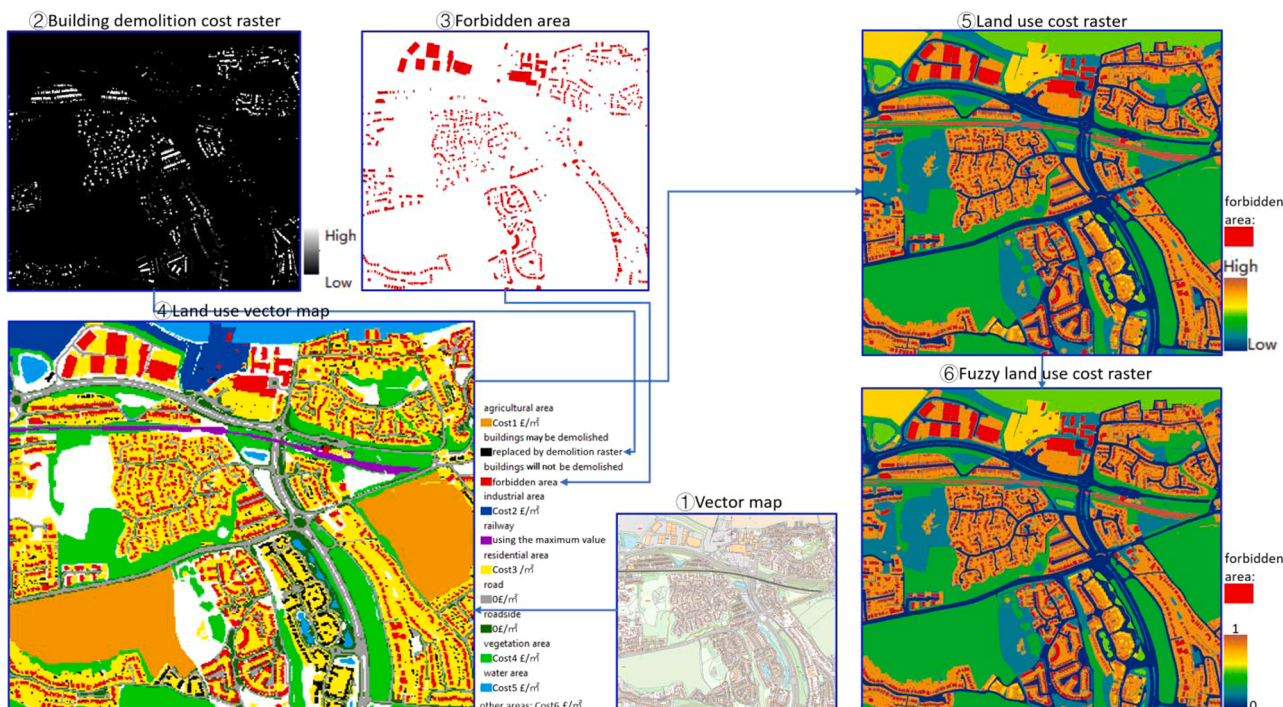


Fig. 3. Establish land use cost raster.

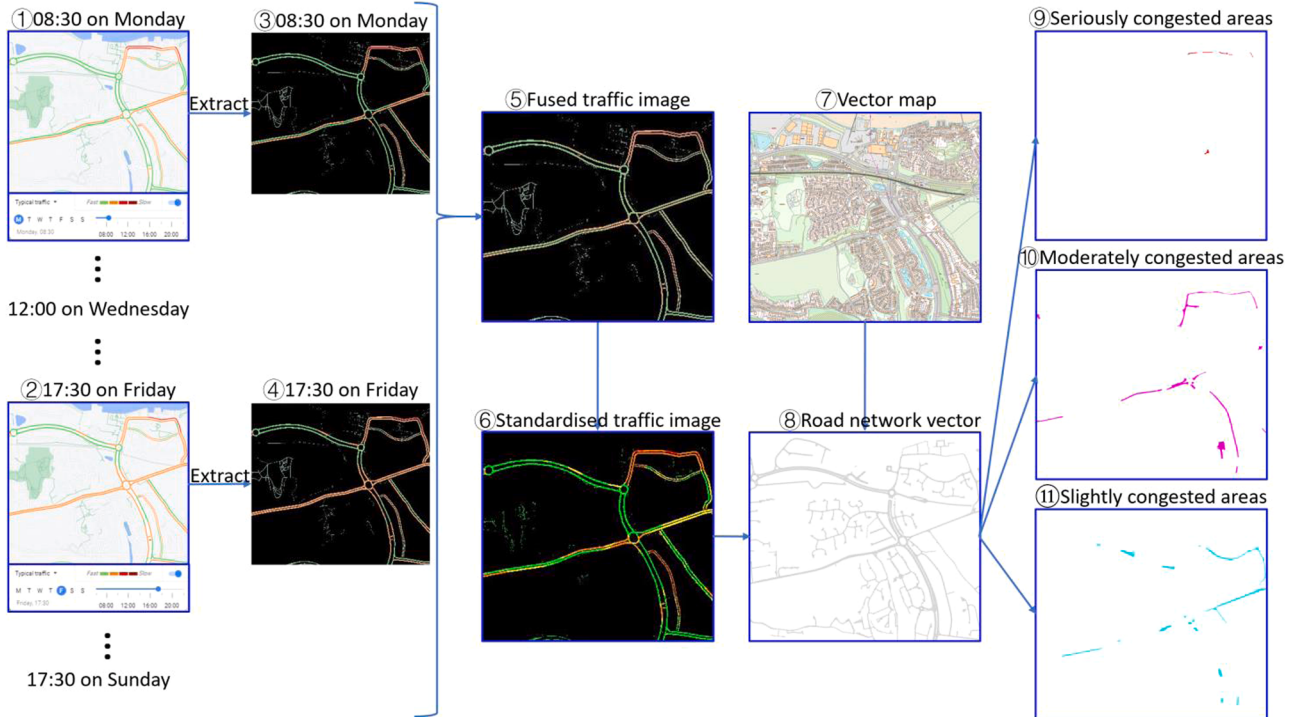


Fig. 4. Extract traffic congestion situations in the target area.

Table 1
Extraction process of the colours representing traffic congestion situations.

Conditions	Processing method	Instructions
$\text{abs}((g(i,j)-b(i,j))/(r(i,j)-b(i,j))) \leq t_1 \text{ and } r(i,j) > b(i,j)$ and $b(i,j) \leq t_4 \text{ and } r(i,j) \leq t_5$	$r_e(i,j)=r(i,j)$ $g_e(i,j)=g(i,j)$ $b_e(i,j)=b(i,j)$	Dark red areas: severely congested keep the original colour
$\text{abs}((g(i,j)-b(i,j))/(r(i,j)-b(i,j))) \leq t_1 \text{ and } r(i,j) > b(i,j)$ and $b(i,j) \leq t_4 \text{ and } r(i,j) > t_5$ $t_1 < (g(i,j)-b(i,j)) / (r(i,j)-b(i,j)) \leq t_2$ and $r(i,j) > b(i,j) \text{ and } g(i,j) > b(i,j) \text{ and } b(i,j) \leq t_4$ $t_2 < (g(i,j)-b(i,j)) / (r(i,j)-b(i,j)) \leq t_3$ and $r(i,j) > b(i,j) \text{ and } g(i,j) > b(i,j) \text{ and } b(i,j) \leq t_4$	$r_e(i,j)=r(i,j)$ $g_e(i,j)=g(i,j)$ $b_e(i,j)=b(i,j)$ $r_e(i,j)=r(i,j)$ $g_e(i,j)=g(i,j)$ $b_e(i,j)=b(i,j)$ $r_e(i,j)=0$ $g_e(i,j)=0$ $b_e(i,j)=0$	Red areas: severely congested keep the original colour Orange areas: moderately congested keep the original colour Yellow areas: represent main road central lines, are changed to black
$\text{abs}((g(i,j)-b(i,j))/(r(i,j)-b(i,j))) \geq t_3 \text{ and } g(i,j) > b(i,j) \text{ and } b(i,j) \leq t_4$ Else	$r_e(i,j)=r(i,j)$ $g_e(i,j)=g(i,j)$ $b_e(i,j)=b(i,j)$ $r_e(i,j)=0$ $g_e(i,j)=0$ $b_e(i,j)=0$	Green areas: no traffic congestion keep the original colour Other areas: represent background, buildings, water areas, other roads, gardens (emerald), parks(emerald), etc. are changed to black

$$\begin{aligned} r_{\text{fused}}(i,j) &= \frac{1}{n} \sum_{k=1}^n r_{e,k}(i,j), \quad g_{\text{fused}}(i,j) = \frac{1}{n} \sum_{k=1}^n g_{e,k}(i,j), \quad b_{\text{fused}}(i,j) \\ &= \frac{1}{n} \sum_{k=1}^n b_{e,k}(i,j) \end{aligned} \quad (5)$$

Then, the road vectors from Section 0 with different traffic congestion situations where they are red, orange and yellow in the corresponding position in the standardised traffic image can be extracted from the network vectors, as shown in ⑨, ⑩, and ⑪ in Fig. 4.

The newly built roads and widened roads are preferred to be planned near the traffic-congested areas. Thus, the Euclidean distance rasters of the seriously, moderately, and slightly congested areas are established to

Table 2
Standardisation process of the fused traffic image.

Conditions	Processing method	Instructions
$\text{abs}((g_{\text{fused}}(i,j)-b_{\text{fused}}(i,j))/(r_{\text{fused}}(i,j)-b_{\text{fused}}(i,j))) \leq t_6 \text{ and } r_{\text{fused}}(i,j) > b_{\text{fused}}(i,j)$ and $g_{\text{fused}}(i,j) < t_9 \text{ and } (r_{\text{fused}}(i,j)+g_{\text{fused}}(i,j)+b_{\text{fused}}(i,j)) > t_{10}$	$r_s(i,j)=1$ $g_s(i,j)=0$ $b_s(i,j)=0$	Severely congested
$t_6 < (g_{\text{fused}}(i,j)-b_{\text{fused}}(i,j)) / (r_{\text{fused}}(i,j)-b_{\text{fused}}(i,j)) \leq t_7$ and $r_{\text{fused}}(i,j) > b_{\text{fused}}(i,j)$ and $g_{\text{fused}}(i,j) > b_{\text{fused}}(i,j) \text{ and } b_{\text{fused}}(i,j) \leq t_9$ $(r_{\text{fused}}(i,j)+g_{\text{fused}}(i,j)+b_{\text{fused}}(i,j)) > t_{10}$	$r_s(i,j)=1$ $g_s(i,j)=0.5$ $b_s(i,j)=0$	Moderately congested
$t_7 < (g_{\text{fused}}(i,j)-b_{\text{fused}}(i,j)) / (r_{\text{fused}}(i,j)-b_{\text{fused}}(i,j)) \leq t_8$ and $r_{\text{fused}}(i,j) > b_{\text{fused}}(i,j)$ and $g_{\text{fused}}(i,j) > b_{\text{fused}}(i,j) \text{ and } b_{\text{fused}}(i,j) \leq t_9$ $(r_{\text{fused}}(i,j)+g_{\text{fused}}(i,j)+b_{\text{fused}}(i,j)) > t_{10}$	$r_s(i,j)=1$ $g_s(i,j)=1$ $b_s(i,j)=0$	Slightly congested
$\text{abs}((g_{\text{fused}}(i,j)-b_{\text{fused}}(i,j))/(r_{\text{fused}}(i,j)-b_{\text{fused}}(i,j))) > t_8$ and $g_{\text{fused}}(i,j) > b_{\text{fused}}(i,j)$ and $b_{\text{fused}}(i,j) \leq t_9$ $(r_{\text{fused}}(i,j)+g_{\text{fused}}(i,j)+b_{\text{fused}}(i,j)) > t_{10}$	$r_s(i,j)=0$ $g_s(i,j)=1$ $b_s(i,j)=0$	No traffic congestion
Else	$r_s(i,j)=0$ $g_s(i,j)=0$ $b_s(i,j)=0$	Other areas are changed to black

represent the preferences for road construction locations, as shown in ④, ⑤, ⑥ in Fig. 5 and Eqs. (6), where x and y denote the position of the target cell and x_i and y_i denote the positions of the cells in the congested areas. Then, according to the Analytic Hierarchy Process (AHP), a pairwise comparison matrix (PCM) is established according to the experts to give weights to Euclidean distance rasters where a_{ij} is the element of the PCM representing the importance compared between two factors (means two Euclidean distance rasters here), as shown in Eqs. (7) (Saaty, 1977). $a_{ij} = 1, 3, 5, 7, 9$ means factor i is the same important, moderately more important, strongly more important, very strongly more important, and extremely more important respectively compared with factor j. 2, 4, 6, 8 are the intermediate values. Then, the eigenvector w of the PCM corresponding to the PCM's largest eigenvalue can be

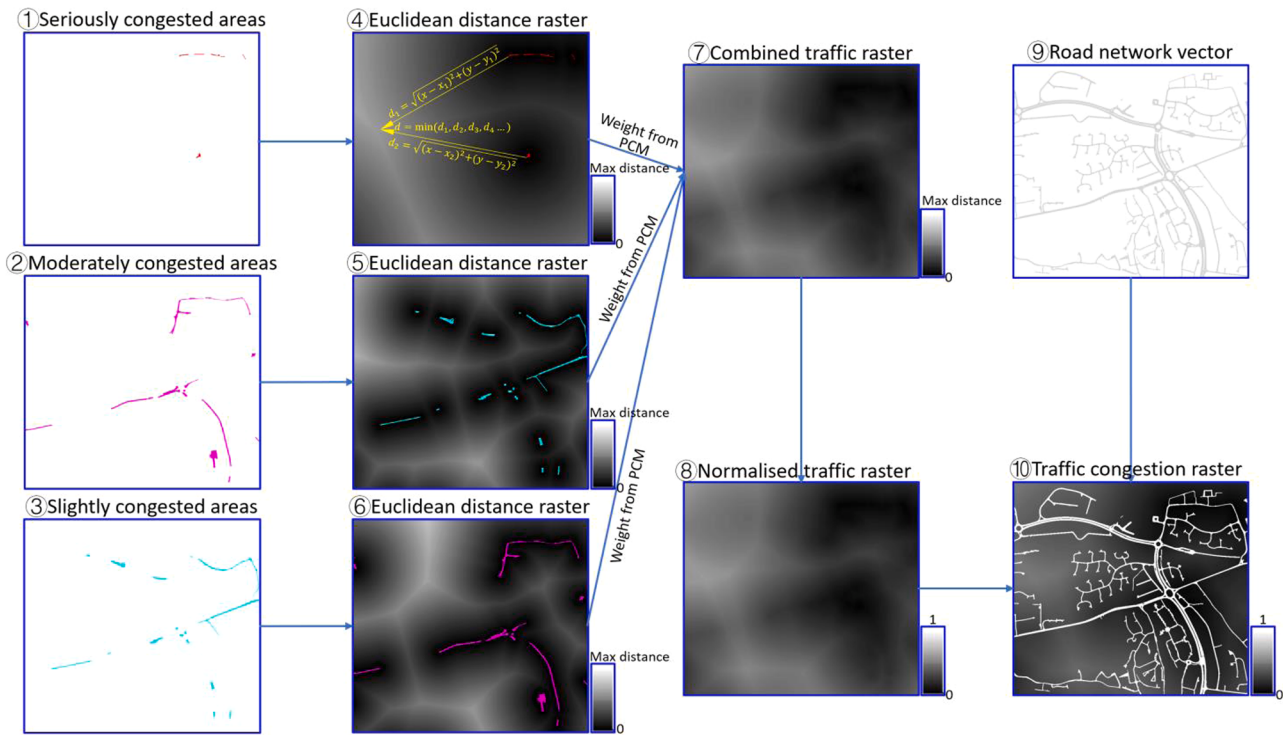


Fig. 5. Establish traffic congestion raster.

calculated and ω_i is the element of ω , as shown in Eqs. (8). Then, the weight ($W(k)$) given to various rasters can be calculated by Eqs. (9) using ω_i . The Euclidean distance rasters of the seriously congested areas should be given the maximum weight. The desired target raster can be obtained by Eq. (10), where $Cell_{target}(i,j)$ and $Cell_k(i,j)$ are the values of cells on the desired target raster and various known rasters, respectively. In this section, $Cell_{target}(i,j)$ are the cells' values on the combined traffic congestion raster (⑦ in Fig. 5), and $Cell_k(i,j)$ are the cells' values on Euclidean distance rasters of different congested areas. Afterwards, the combined traffic congestion raster is normalised using Eq. (11), as shown in ⑧ in Fig. 5. If the planned road is entirely on the existing road network areas, it means that the planned road makes full use of established roads in these areas, where there are no newly constructed or widened roads to alleviate traffic congestion. Thus, in the areas of the road network (⑨ in Fig. 5), based on the normalised raster, the values will be changed to 1 in the traffic congestion raster (⑩ in Fig. 5).

$$d = \min \left(\sqrt{(x - x_i)^2 + (y - y_i)^2} \right) \quad (6)$$

$$\begin{aligned} PCM &= \begin{bmatrix} a_{11} & \dots & a_{1n} \\ \vdots & \ddots & \vdots \\ a_{n1} & \dots & a_{nn} \end{bmatrix}, a_{ii} = 1, a_{ji} = \frac{1}{a_{ij}}, a_{ij} \neq 0, a_{ij} \\ &= \frac{1}{2}, \frac{1}{3}, \dots, \frac{1}{9}, \text{ or } 1, 2, \dots, 9 \end{aligned} \quad (7)$$

$$\omega = \begin{bmatrix} \omega_1 \\ \vdots \\ \omega_k \\ \vdots \\ \omega_n \end{bmatrix} \quad (8)$$

$$W(k) = \frac{\omega_k}{\sum_{k=1}^n \omega_k} \quad (9)$$

$$Cell_{target}(i,j) = \sum_{k=1}^n W(k) Cell_k(i,j) \quad (10)$$

$$Cell_{normalised}(i,j) = \frac{Cell_{target}(i,j)}{\max(Cell_{target})} \quad (11)$$

2.3. Noise consideration

On the one hand, the noise impact after the construction and widening of the planned road on the buildings should be considered. On the other hand, the existing noise impact should be considered. If the existing noise impact is already severe in an area, the impact from a newly constructed or widened road on the buildings in this area can be very slight. Thus, the increase in noise after the construction and widening of the planned road compared to the existing noise needs to be considered. The existing digital noise data in the research area can be downloaded from government statistics in GIS format (Department for Environment Food and Rural Affairs, 2019). Then, the noise dB after the construction and widening of the planned road on the buildings is calculated as a line noise source according to the Calculation of Road Traffic Noise (CRTN) model, as shown in Fig. 6 (Sheng et al., 2015; Wang et al., 2017). For a road on each side, there are two to four lanes. A three-lane carriageway is used for noise estimation, and the size of each component is according to the UK highway design standard (Highways England, 2021). The effective noise source line is assumed 3.5m inwards from the outer edge of the carriageway. The noise decibel value (dB) is calculated using the distance from the central alignment of the road (D) and based on the noise dB (L_0) at the position with the standard distance (10m) from the outer edge of the carriageway (Building 2). The distance refers to the shortest distance between the central line and the corresponding point on the building. If D is smaller than (10+12.75)m, the noise dB is regarded as the value at the position with the standard distance and the building is highly likely to be demolished in the real circumstance (Building 1). If D is no smaller than (10+12.75)m (Building 2 and Building 3), the noise dB can be calculated according to Eq. (12).

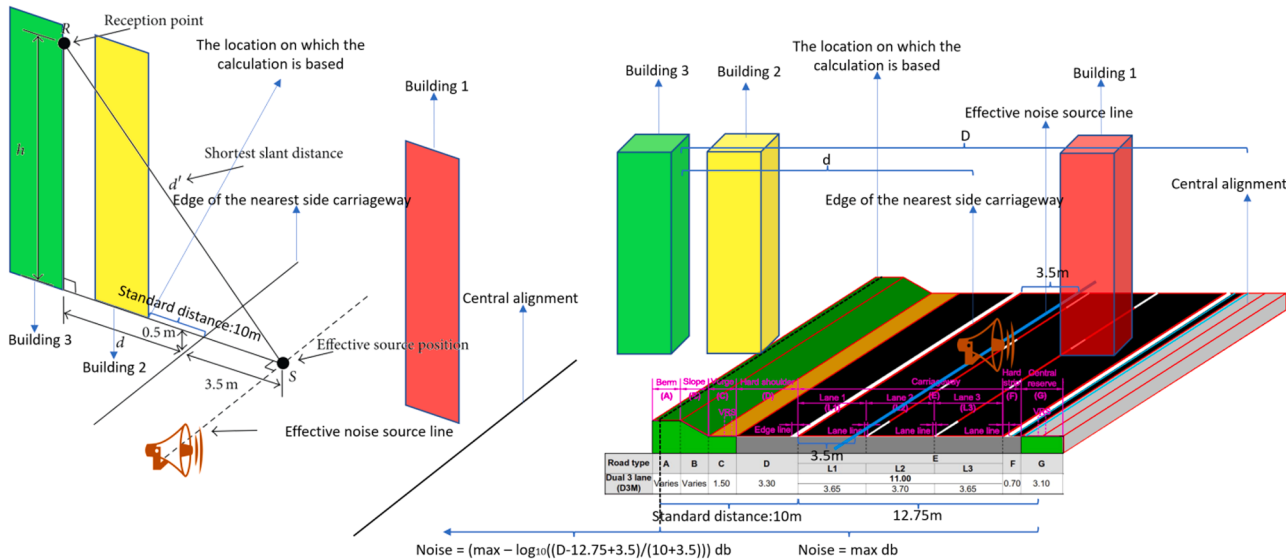


Fig. 6. Calculation of the noise after the construction and widening of the planned road.

$$L = \begin{cases} L_0 & , D < 22.75 \\ L_0 - 10\log_{10}\left(\frac{D - 12.75 + 3.5}{10 + 3.5}\right), & D \geq 22.75 \end{cases} \quad (12)$$

Since the position of the planned road cannot be determined and the buildings are fixed, it assumes that noise comes from a building to influence the road. Conversely, the noise can represent the noise impact of the planned road on buildings. Thus, the buildings' Euclidean distance rasters (BED raster) in the target research areas are calculated (① in Fig. 7), and the raster representing the noise impact from the newly constructed and widened road on the buildings called noise impact raster (NI raster) (② in Fig. 7) can be calculated based on the BED raster according to Eq. (12), where D uses the value of each cell on the BED raster and L represents the value of each cell on the NI raster. The raster representing the existing noise dB distribution of the research area

called the existing noise raster (EN raster) (④ in Fig. 7) can be built in GIS according to government statistics. The final noise raster can be calculated according to the difference between the NI raster and BED raster. According to Environmental Health Criteria of Noise from World Health Organization (WHO), in residential areas where the general daytime noise exposure is below 55 dB(A) L_{eq} , there will be few people seriously annoyed by the noise, and the noise has no apparent damage to human health if noise is below 70 dB (World Health Organization, 1980). Thus, the noise raster (④ in Fig. 7) can be created according to Table 3.

2.4. Air pollutant consideration

Sustainable urban road planning should consider air pollutants like $PM_{2.5}$, PM_{10} , NO_2 , SO_2 , CO , and O_3 . In addition, carbon emission (CO_2)

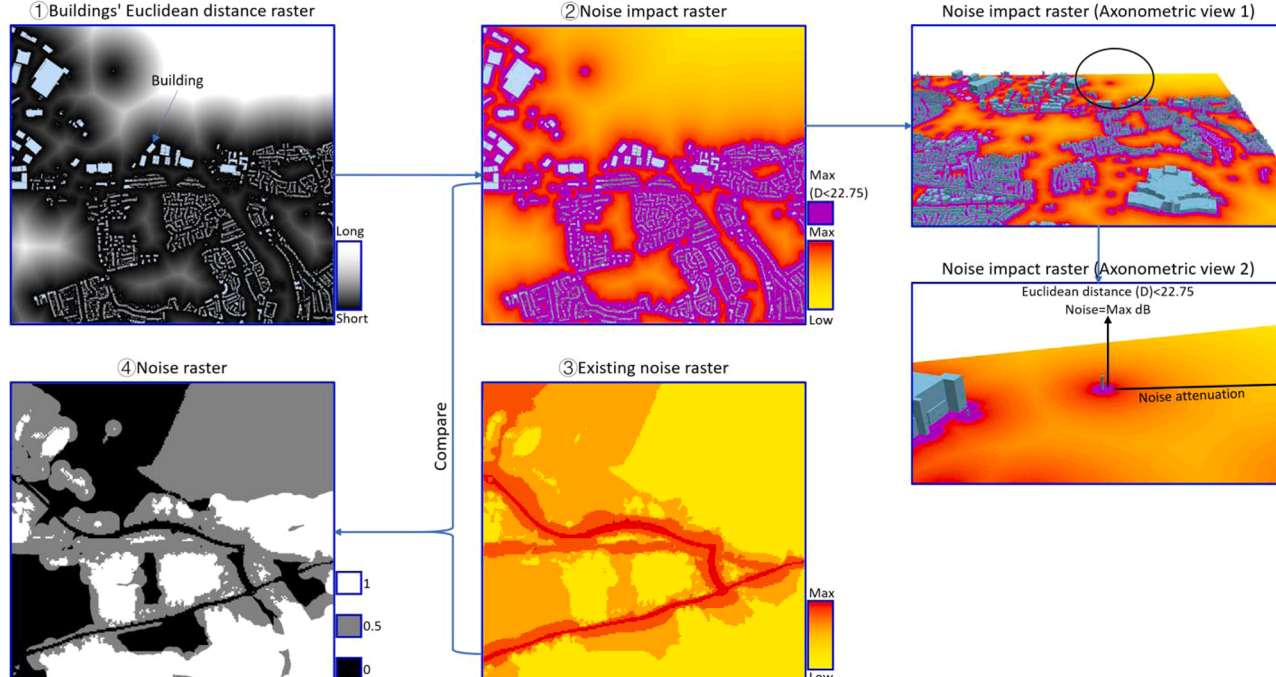


Fig. 7. Workflow of creating the noise raster.

Table 3

Create a noise raster according to the existing noise raster and noise impact raster.

Existing noise raster	Noise impact raster	Noise raster	Instruction
<55dB	<55dB	0	Slight influence or no influence
<55dB	≥55dB and <70dB	0.5	Moderate influence
<55dB	≥70dB	1	Severe influence
≥55dB and <70dB	<55dB	0	Slight influence or no influence
≥55dB and <70dB	≥55dB and <70dB	0	Slight influence or no influence
≥55dB and <70dB	≥70dB	0.5	Moderate influence
≥70dB	<55dB	0	Slight influence or no influence
≥70dB	≥55dB and <70dB	0	Slight influence or no influence
≥70dB	≥70dB	0	Slight influence or no influence

also should be considered. Though this research only presents three main pollutants: PM_{2.5}, PM₁₀, and NO₂, the proposed method in this section also can be employed in other air pollutants and carbon emissions. The predicted air pollutant concentration after the newly constructed or widened road in the target area is also calculated based on the air pollutant concentration (C₀) 10m from the outer edge of the carriageway. The sizes of the road components and the standard positions for the air pollutant calculation method are similar to Fig. 6 in Section 0. Since the air pollutant concentration represents the annual average concentration in this area, the wind direction, speed, temperature, and plume components at a specific time are not considered. In addition, this research only considers horizontal dispersion in general. Thus, this research only considers lateral plume meander and assumes that the plume has an equal probability of moving in any direction. Then, the air pollutant concentration can be estimated by Eq. (13), and the concentration is inversely proportional to the distance (x) to the pollutant source (Cimorelli et al., 2005; Snyder et al., 2013). Thus, the raster representing air pollutant concentration (C) after the construction and widening of the planned road called new concentration raster (NC raster) (② in Fig. 8) can also be calculated according to the buildings' Euclidean distance raster (① in Fig. 8) and Eqs. (14). In addition, the

raster called the existing concentration raster (EC raster) (④ in Fig. 8), representing the existing air pollutant concentration, is established according to online data and government statistics.

$$C = \frac{1}{2\pi x} \quad (13)$$

$$C = \begin{cases} C_0, & D < 22.75 \\ C_0 \left(\frac{10 + 3.5}{D - 12.75 + 3.5} \right), & D \geq 22.75 \end{cases} \quad (14)$$

The annual air quality guideline (AQG) levels and interim target levels for PM_{2.5}, PM₁₀, and NO₂ according to WHO are shown in Table 4 (World Health Organization, 2021). The hazard rates (HR) of non-accidental mortality in a population due to long-term exposure to PM_{2.5}, PM₁₀, and NO₂ have a linear increase of 1.08, 1.04, and 1.02 per 10 µg/m³, respectively. At higher concentrations, the increase of HR by concentration may no longer be linear. If mortality in a population exposed to air pollutants at the AQG level is arbitrarily set to 100, then the mortality in populations at interim target 1, 2, 3 and 4 levels are shown in Table 4. Since the impact of the same concentration of different kinds of air pollutants on citizens is different, non-accidental mortality is used as a unified criterion for different kinds of air pollutants. The NC raster and EC raster are reclassified. Each cell value is changed to the difference between its corresponding mortality at different concentration levels and 100 (at AQG Level), according to Table 5. The reclassified rasters are called new mortality raster (NM raster) (③ in Fig. 8) and existing mortality raster (EM raster) (⑤ in Fig. 8). Then mortality increase raster (MI raster) is established by the difference between the NM raster and EM raster (⑥ in Fig. 8). If the difference value is negative, it will be changed to zero. Then, the MI rasters are combined according to their weights to obtain the combined mortality raster. The value of each cell on the combined mortality raster is divided by the maximum value on the combined mortality raster can obtain the final air pollutant raster, as shown in Fig. 9.

2.5. Construction cost consideration

Areas with appropriate width (W_{buffer}) outward from the road edge are regarded as road buffer areas, representing road widening areas, as shown in Fig. 10. This research sets the W_{buffer} to the standard width of two additional lanes widening from two lanes to four lanes on one side. For example, according to the UK highway design standard, the W_{buffer}

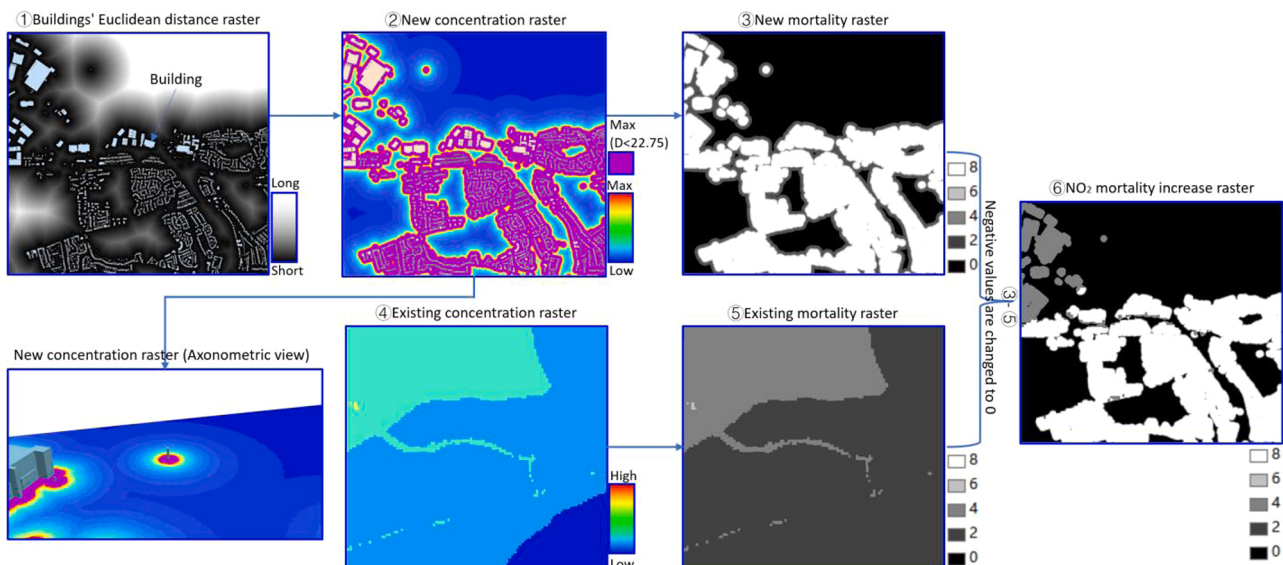


Fig. 8. Workflow of creating mortality increase raster.

Table 4

Annual AQG levels and interim target levels for air pollutants according to WHO.

Recommendation	PM _{2.5} ($\mu\text{g}/\text{m}^3$)	PM _{2.5} mortality	PM ₁₀ ($\mu\text{g}/\text{m}^3$)	PM ₁₀ mortality	NO ₂ ($\mu\text{g}/\text{m}^3$)	NO ₂ mortality
Interim target 1	35	124	70	122	40	106
Interim target 2	25	116	50	114	30	104
Interim target 3	15	108	30	106	20	102
Interim target 4	10	104	20	102		
AQG Level	5	100	15	100	10	100

Table 5

Reclassify the new and existing concentration raster according to mortality.

PM _{2.5} ($\mu\text{g}/\text{m}^3$)	Values in mortality raster	PM ₁₀ ($\mu\text{g}/\text{m}^3$)	Values in mortality raster	NO ₂ ($\mu\text{g}/\text{m}^3$)	Values in mortality raster
>35	32	>70	30		
>25 and ≤35	24	>50 and ≤70	22	>40	8
>15 and ≤25	16	>30 and ≤50	14	>30 and ≤40	6
>10 and ≤15	8	>20 and ≤30	6	>20 and ≤30	4
>5 and ≤10	4	>15 and ≤20	2	>10 and ≤20	2
≥0 and ≤5	0	≥0 and ≤15	0	>0 and ≤10	0

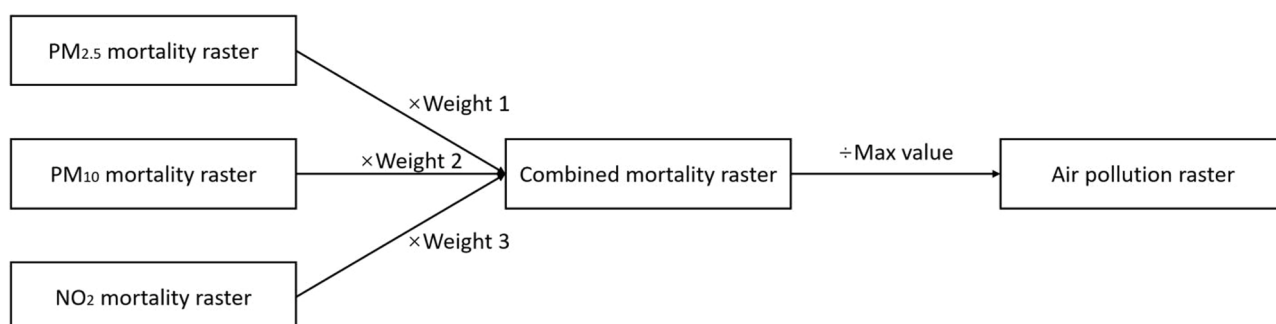
can be set to 7.4m (① in Fig. 10) (Highways England, 2021). However, if the road is wide enough, such as a standard two-way eight-lane road, it should not be widened. After that, different types of areas for road construction can be obtained, such as buildings that may be demolished, railways, roads, road buffer areas (roads can be widened), special soil, water areas, and other areas (④ in Fig. 11). Then, a PCM is given to various areas by experts. Bridges and tunnels should be built in the railway and water areas. Thus, the construction costs are high. In demolition areas, buildings should be demolished, and demolition waste and the site need to be treated. Thus, their construction costs are relatively high. The construction costs in the special soil areas follow behind. In other areas, the construction costs refer to the costs of the newly built road in regular areas, which are moderate. In the road buffer areas (roads can be widened), the construction costs are lower than the newly built roads in regular areas. In road areas, there are no newly built roads or widened roads. There are mainly some road maintenance costs, which are much lower. After the PCM is determined, the construction cost raster can be obtained (⑥ in Fig. 11), and the cells' values can be calculated by Eqs. (15), where ω_k is the element of the eigenvector of the PCM corresponding to its largest eigenvalue, and k refers to a type of area for road construction. The road buffer areas (roads cannot be widened) are for later use where the cells' values are set to 1 in the overall cost raster in Section 2.3 (③ in Fig. 11).

$$\text{Cell}_k(i,j) = \frac{\omega_k}{\max(\omega_k)} \quad (15)$$

2.6. New road alignment planning method considering road width and road widening

After that, the overall cost raster should be created, as shown in Fig. 12. An appropriate PCM is provided by the experts to give weights to the different rasters to establish the semi-finished overall cost raster. Based on the semi-finished overall cost raster, other forbidden areas (landmarks, nature reserves, cemeteries, cultural heritage areas, etc.) are set on the overall cost raster. In addition, values on the buffer areas of the main roads, which cannot be widened, are set to 1. Then, the planned road will occupy the road buffer areas (roads cannot be widened) as less as possible. After that, the start point cell and the end point cell on the overall cost raster and the width of the planned road are set. Then, the road alignment planning can be conducted on the overall cost raster, considering road width and widening.

Based on the least-cost path algorithm on the raster (Douglas, 1994), Dijkstra's shortest path algorithm (Dijkstra, 1959), and the least-cost wide path algorithm (Shirabe, 2016), we enrich and employ the algorithm to be implemented in road alignment planning in the built environment, which can consider road width and road widening in the limited space in the city. On the raster, each target cell with its corresponding occupied cells forms the brush head, which can be defined in Fig. 13. The target cell refers to the cell in the raster, which is focused on in the current step in the calculation process. For each target cell, an $n \times n$ cell group is drawn. In this research, n is set to a positive odd number. The target cell is the centre cell, as shown in ① in Fig. 13. A $d \times d$ cell group at four corners are selected as corner cells, as shown in ② in Fig. 13. Then, four diagonal lines of all the $d \times d$ cell groups are drawn. If a cell is outside or touched by the diagonal line, the cell is regarded as a deleted cell, as shown in ③ in Fig. 13. After the deleted cells are removed, the remaining cells are the target cell with its occupied cells, regarded as a brush head drawing the least-cost wide path, as shown in ④ in Fig. 13. To ensure the brush head can draw the path with a similar width in every direction, the diagonal length of the brush head should be similar to the side length. There are two diagonal lengths of the brush head. The longer one is $\sqrt{2}(n-d)L$ and the shorter one is $\sqrt{2}(n-d-1)L$, where L is the side length of a cell. Thus, a relation can be obtained in Eq. (16) and the d value can be determined by Eq. (17), where the floor denotes rounding down a number into an integer. Image ④-⑧ in Fig. 13 provide several examples of the brush head.

**Fig. 9.** Workflow of creating air pollution raster.

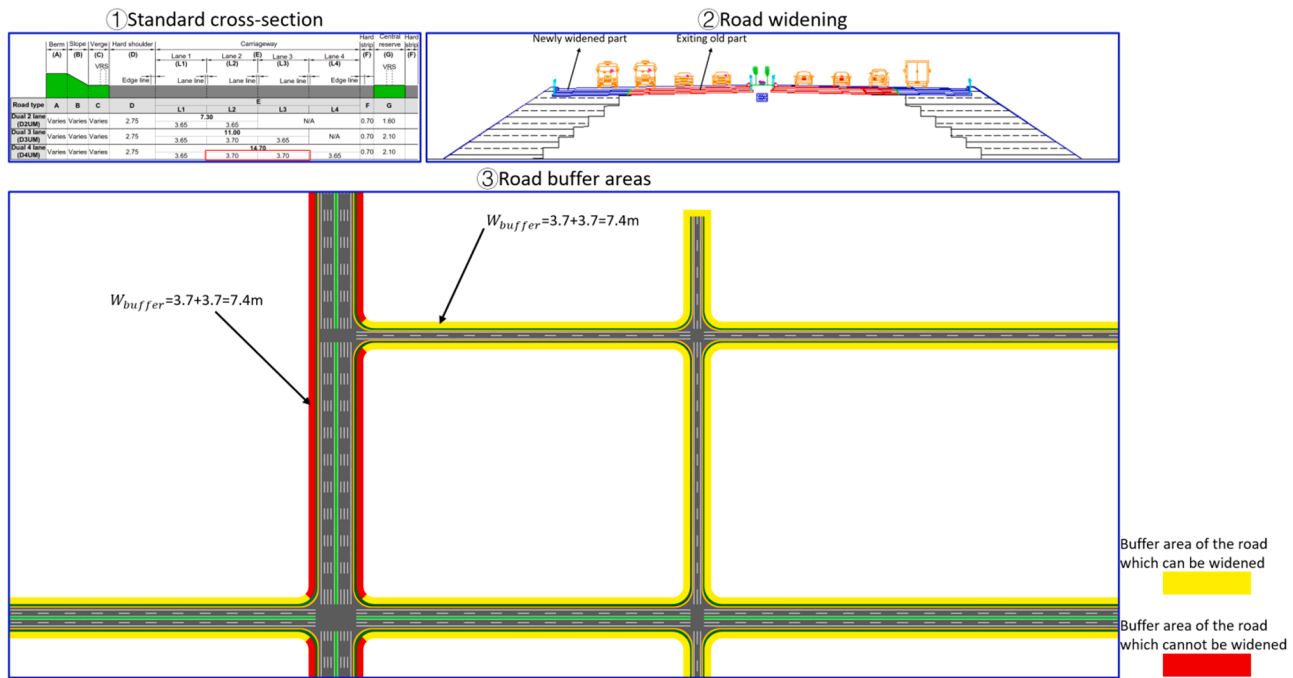


Fig. 10. Road widening and road buffer areas.

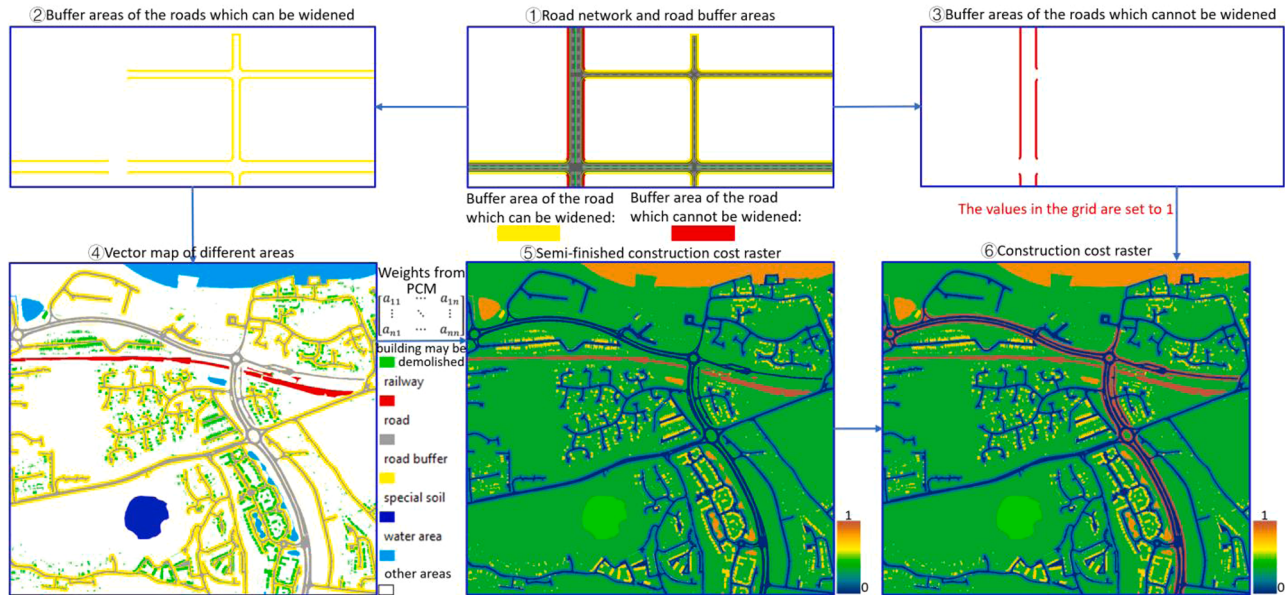


Fig. 11. Construction cost raster considering both new road construction and existing road widening.

$$\sqrt{2}(n-d)L < n \times L < \sqrt{2}(n-d-1)L \quad (16)$$

$$d = \text{floor}\left(\frac{(2 - \sqrt{2})n}{2}\right) \quad (17)$$

The definition of the forbidden cells on a raster is shown in Fig. 14. Forbidden cells cannot be occupied by the brush head. Since a brush head has multiple cells, extended forbidden cells emerge, which can be occupied by the occupied cells and cannot be occupied by the target cell. In addition to forbidden cells, the raster's edge can also cause extended forbidden cells, where target cells cannot arrive at these areas. Otherwise, some occupied cells of the brush head will go beyond the raster.

On the cost raster (① in Fig. 15), the start point cell and end point

cell can be set. Several cells with infinite high costs ($1e9$) represent forbidden areas. The accumulated cost (AC) of a cell denotes the accumulated cost from the start point, and the cost distance raster describes the least accumulated cost (LAC) of each cell from the start point through the optimal path. The initial cost distance raster is shown in ② in Fig. 15, where the accumulated cost of the start point cell is the sum of the values (172 in ② in Fig. 15) of all the cells of the brush head on the cost raster when the target cell of the brush head is on the start point, and other cells are $1e9$. The current target cell of the brush head, which is focused on, is called the focused target cell (⑦ in Fig. 15). At this time, the AC of the focused cell of the current cost distance raster is its LAC. Then, the brush head on the focused target cell moves in eight directions (③-⑪ in Fig. 15), respectively, and the target cells at the new positions

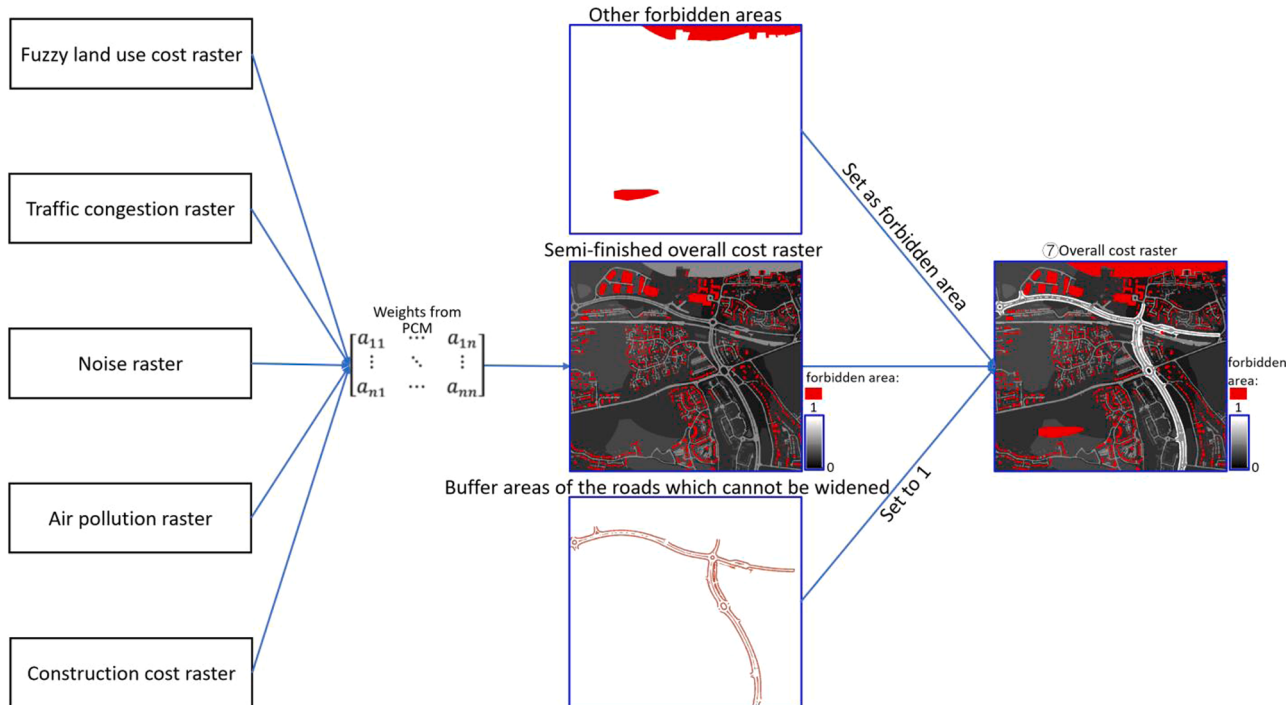


Fig. 12. Establish the overall cost raster.

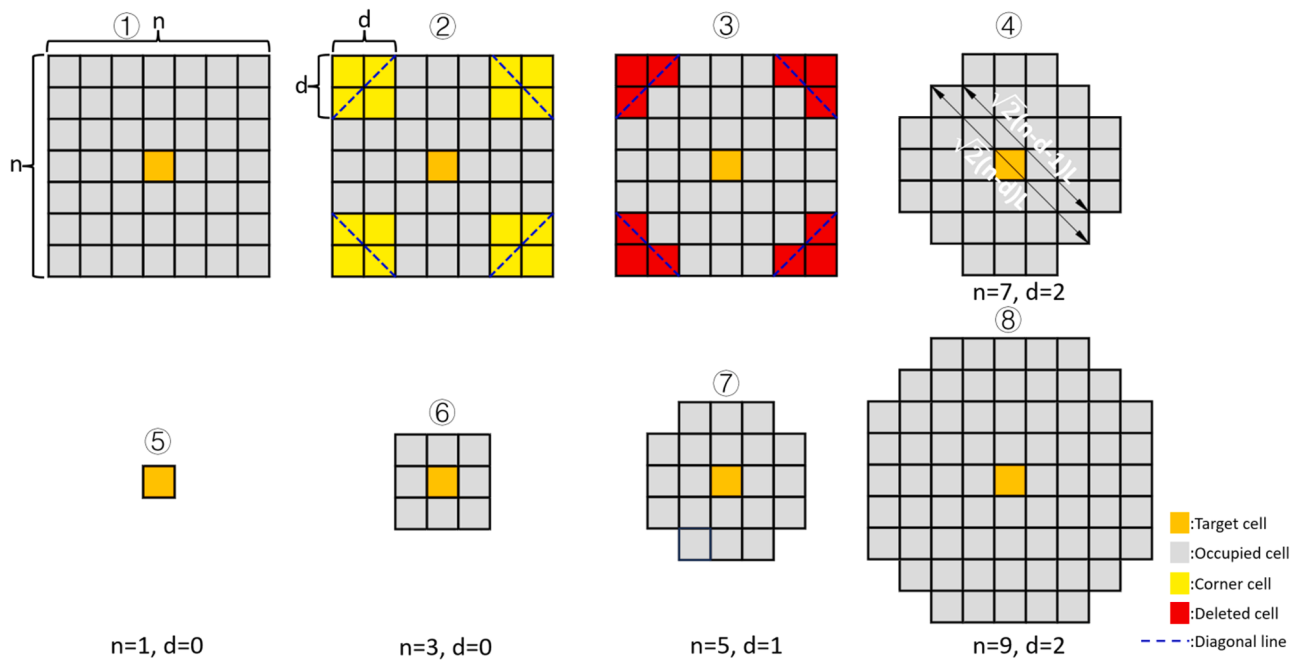


Fig. 13. Definition of the brush head.

are called the neighbour cells of the target cell. Then, the pending accumulated cost (PAC) of the neighbour cells, which is the sum of the AC of the focused target cell (172 in ② in Fig. 15) and the corresponding values of the added cells. The calculation process is shown in ② in Fig. 15, and the results are shown in ③ in Fig. 15. Then, for each target cell in the eight directions, if its PAC is smaller than its current AC in the cost distance raster, its AC will be replaced by its PAC. All the neighbour cells of the current and previous focused cells are called active cells. After that, among all the active cells, the cell with the lowest AC in the current cost distance raster is selected as a new focused cell to replace

the former focused cell for the further and similar calculation process and the former focused cell is marked as a visited cell which will not be revisited. Thus, the cost distance raster is continuously updated by the iterative calculation process (④, ⑤, and ⑥ in Fig. 15) until all the cells except for the forbidden cells and extended forbidden cells to obtain the final cost distance raster (⑦ in Fig. 15). After that, for each target cell from the end point, find its neighbour cell (eight directions) with the least AC in the final cost distance raster and the neighbour cell with the least AC is regarded as the new target cell for the next step in the continuous finding process until the target cell is the start point. Finally,

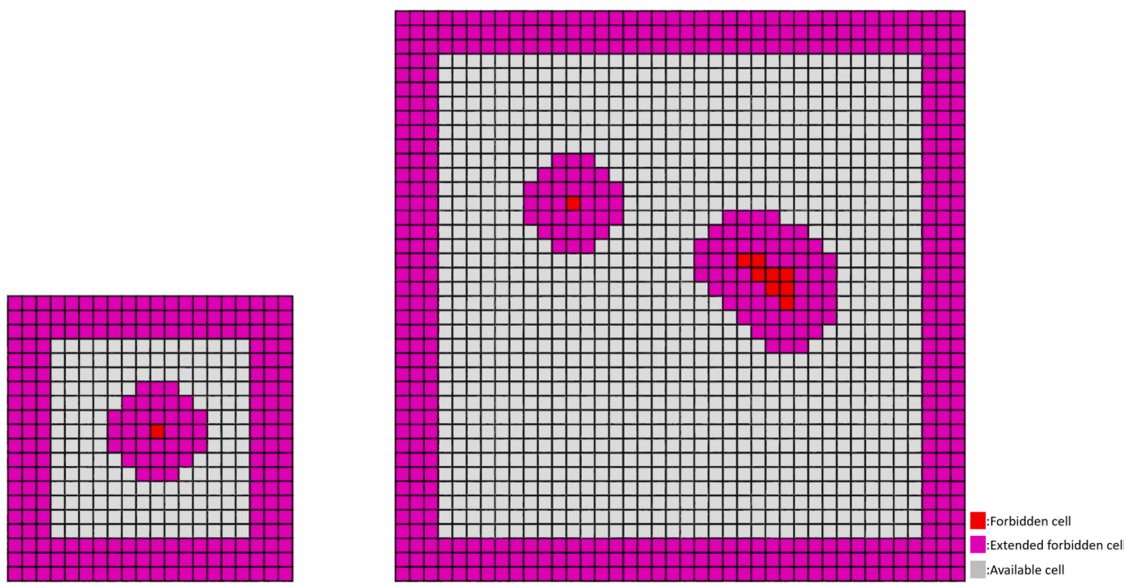


Fig. 14. Definition of forbidden cells.

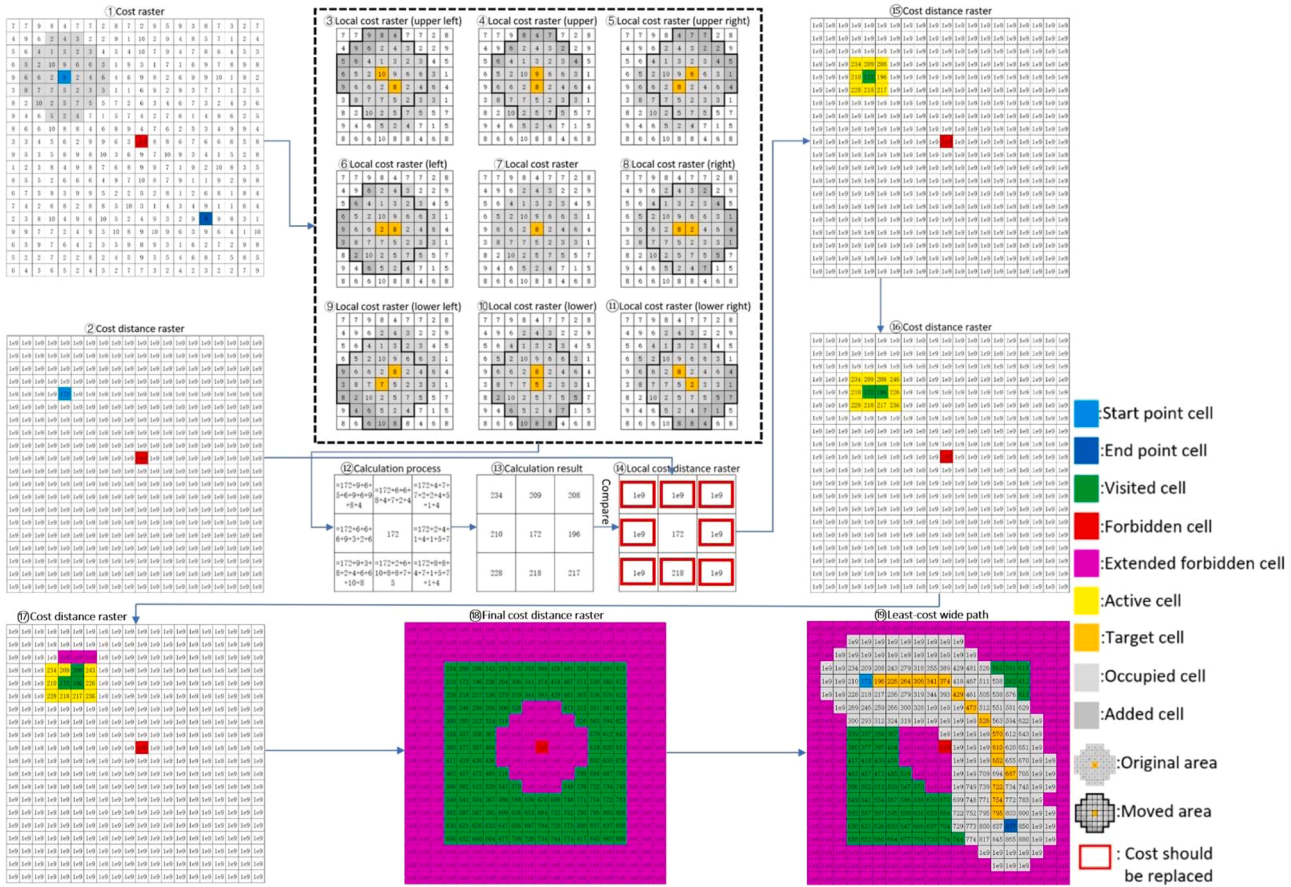


Fig. 15. Least-cost wide path algorithm on the raster.

all the target cells and their occupied cells can form the least-cost wide path (⑩ in Fig. 15).

Based on the algorithm and definitions above, there are several circumstances, as shown in Fig. 16. If the planned wide road alignment goes through the area without roads and is not adjacent to an existing road, it is a newly built section. If the wide alignment coincides with an

old road and is not wider than the old one, it is a section that fully utilises the old road. Only some maintenance and pavement stitching work needs to be done in these sections. If the wide alignment goes along an existing old road and is beyond the old road on both sides, it is a road-widening section on both sides. If the wide alignment goes along an existing old road and is beyond the existing old road on one side, it is a

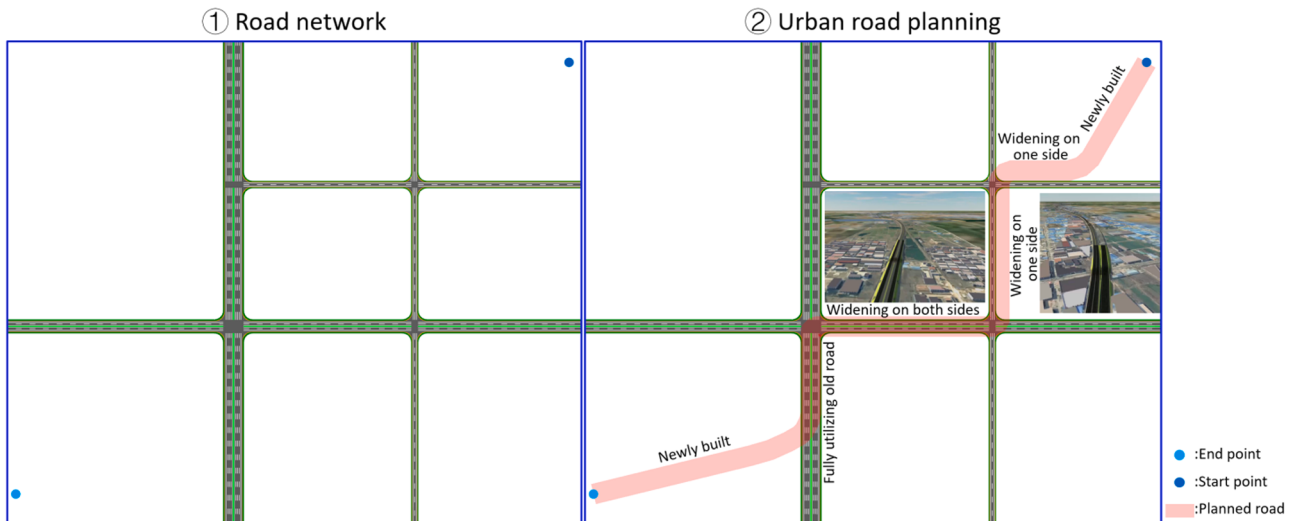


Fig. 16. Road alignment planning in the built environment using the least-cost wide path algorithm.

road-widening section on one side.

3. Case study

3.1. Introduction of the case study

The target research area is located in Dartford District of Kent County, which is to the southeast of London, as shown in the red box in Fig. 17. The east-west length of the target research area is 3993.600m, and the north-south length is 3994.100m. The cell size of the raster is 0.1m and the raster size is 39936×39941 during the raster processing and calculating. The cell size of the final overall raster is 2m and the raster size is 1997×1997 during the alignment planning process. Dartford District is one of the local authority areas with the most development potential in the UK. Its built-up area is connected to London's built-up area. London's ring highway (A282 connected to M25) passes through its city area. The population size in Dartford has increased by 20.0%, from around 97,400 in 2011 to 116,800 in 2021. This is much higher than the overall increase for England (6.6%) (Office

of National Statistics, 2021). There are many residential buildings, a large hospital, a huge shopping centre, and green spaces in the area. The River Thames is in the north of the area, and several warehouses and industrial sites are on the river bank. A2 and A282 highways intersect in this area, which are two-way eight-lane highways and too wide to be widened. Dartford District is divided into the east and west areas by the A282 highway. If citizens want to travel between the two areas, they have to go through A2 and A282 or local road networks. Traffic congestions frequently occur in the area. Thus, in addition to the existing local road network, a new local road needs to be planned from the northwest to the southeast of the area to link the east and west areas. In this way, residents in the west area can easily travel to and from the hospitals and shopping centres in the east area. The start point is (555093.3, 175687.1), and the end point is (558801.3, 172321.1) in the OSGB36 National Grid system.

3.2. Data processing and cost rasters considering various factors

DSM, DTM, and vector map are downloaded from a Digimap (Dig-

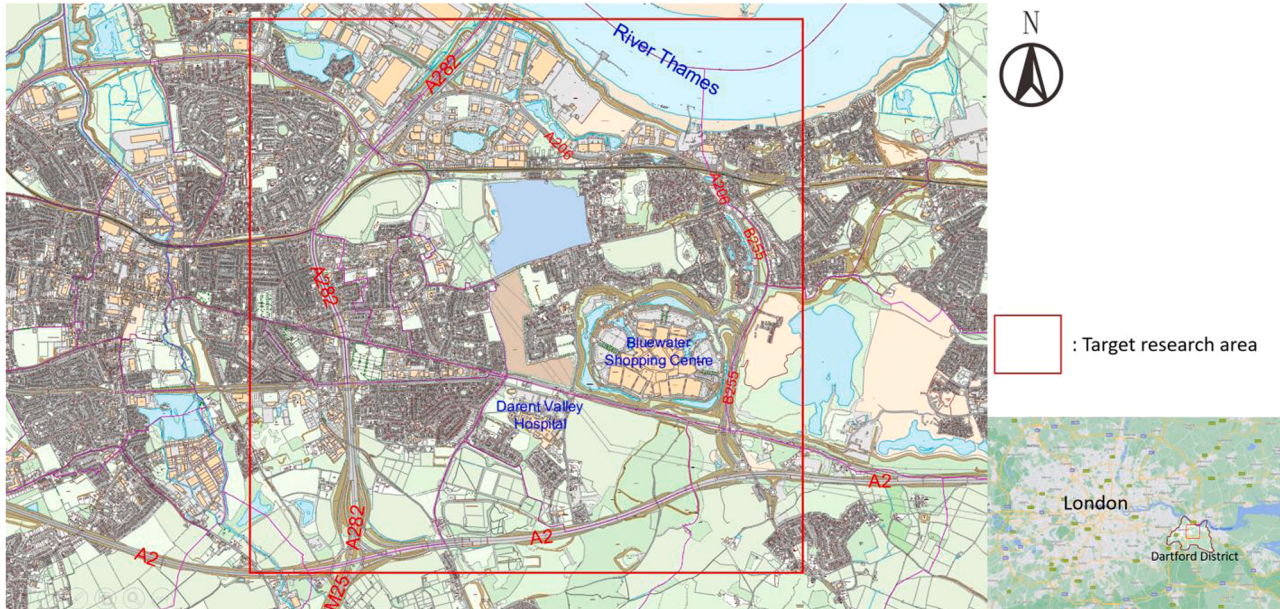


Fig. 17. Target research area.

imap 2022), and DDM, road network can be produced, as shown in Fig. 18. W_{buffer} of the road buffer area is set to 7.4m (3.7m+3.7m) (Highways England, 2021). The traffic congestion screenshot processing and alignment planning algorithms are developed in the Matlab R2020b. ArcMap 10.0 and QGIS desktop 3.22.5 are employed for raster and vector data processing.

The fused and standardised traffic images can be generated based on the traffic congestion screenshots from Google Maps, as shown in Fig. 19. The parameters in Section 0 for digital image processing are presented in Table 6. Then, the areas with different traffic congestions can be extracted to produce traffic congestion rasters, as shown in Fig. 20. Euclidean distance rasters are combined into the combined traffic raster according to the weights from the PCM(traffic), as shown in Table 7. The normalised traffic raster can be calculated according to Eqs. (11), and values in the road network area are set to 1 to get the traffic congestion raster.

The buildings' digital twins are built from the downloaded map data, as shown in ① and ② in Fig. 21. If a building's total area A in Eqs. (1) is larger than the threshold $T_1=100\text{m}^2$, the building will not be demolished because its demolition costs may be very high. According to government statistics, the latest average property price per m^2 in Dartford that can be obtained was 3689 £/ m^2 in 2016 (Office for National Statistics, 2017). In addition, the average overall price of a property in Dartford each month in different years can be obtained (HM Land Registry Open Data, 2021), as shown in Fig. 22 and Table 8. In the case study, the most recent land use values data that can be obtained is for April 2019. Thus, all the data used in the case study are based on the data in April 2019. Then, the average property price per m^2 in April 2019 can be calculated by Eq. (18), where P denotes the average overall price of a property, p denotes the average property price per m^2 , and other P and p at different times are expressed in Table 8. After that, the $C_{demolition}$ of each building that may be demolished is estimated by Eqs. (2), where p uses $p_{April 2019}$ (3894.79£/ m^2). According to the UK policy, for the amount of home loss payment, the owners of a freehold or a lease with at least three years unexpired in England are entitled to 10% of the market value of their interest. In addition, the compensations also should consider disturbance payments and rehousing. The claim for the

disturbance payments can include the costs incurred in acquiring a replacement property (but not the cost of the property itself) and the costs of moving into the property. (Department for Communities and Local Government, 2021). In the case study, the compensations for the disturbance and rehousing are estimated to be 10% of the property's market value. Accordingly, the μ in Eqs. (2) is set to 1.2 in the case study. Then, the building demolition cost raster, and forbidden areas (building that will not be demolished) can be established (③ and ④ in Fig. 21).

$$P_{April 2019} = \frac{12 \cdot p_{2016} \cdot P_{April 2019}}{\sum_{i=January}^{December} P_i, 2016} \quad (18)$$

In addition to building demolition costs, various land values in Dartford in April 2019 can be obtained from Ministry of Housing Communities and Local Government (2019), as shown in ⑤ in Fig. 21. However, the land values of the vegetation areas, water areas, and other areas cannot be obtained, which are estimated and given values around the values of agricultural areas, approximately. The land values are used to represent the land use cost. The land use costs for roads and roadsides are zero since the lands have already been used for roads. Since the maximum building's total area A of the buildings that may be demolished is $T_1=100\text{m}^2$, in the case study, a standard two-storey building (3.2*2m high) with a total area of 100 m^2 is assumed to calculate the threshold T_2 in Eqs. (3). Thus $T_2=2 \cdot 1.2 \cdot 2 \cdot 3894.79=18694.99\text{£}/\text{m}^2$, according to Eqs. (2). In this step, for the convenience of calculation, the land use cost of the forbidden areas is set to the value of residential areas (410£/ m^2) temporarily and will be set as forbidden areas in the overall cost raster. Then the fuzzy land use cost raster can be calculated, as shown in ⑥ in Fig. 21.

The noise distribution in the target research area is obtained from government statistics, as shown in ① and ② in Fig. 23 (Department for Environment Food and Rural Affairs, 2019). This research considers the annual average road and railway noise levels for the 16-hour period between 07:00-23:00 as the existing noise raster. Based on the data, the L_0 in Eqs. (12) is set to 75 dB. According to the method in Section 0, the calculation results for the noise raster are shown in Fig. 23. The original PM_{2.5}, PM₁₀, and NO₂ concentrations in the target air are shown in ③, ④, and ⑤ in Fig. 24 (Cambridge Environmental Research Consultants,

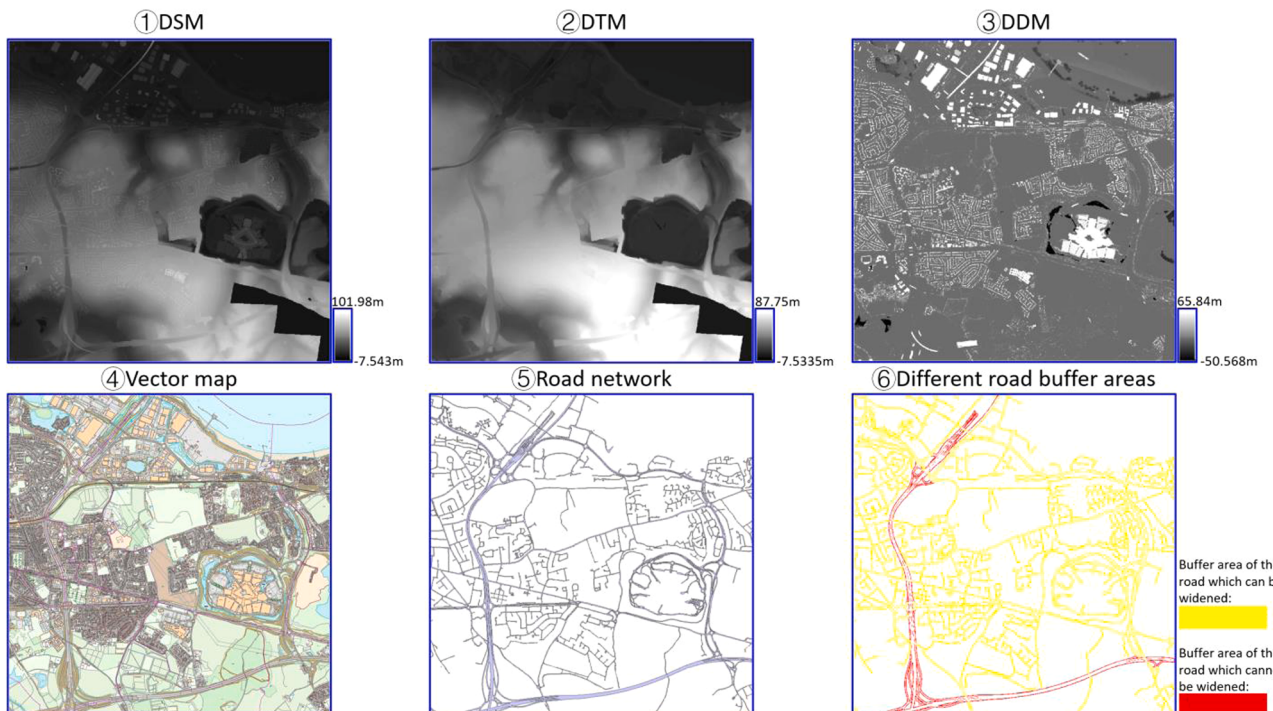


Fig. 18. Map data and data processing.

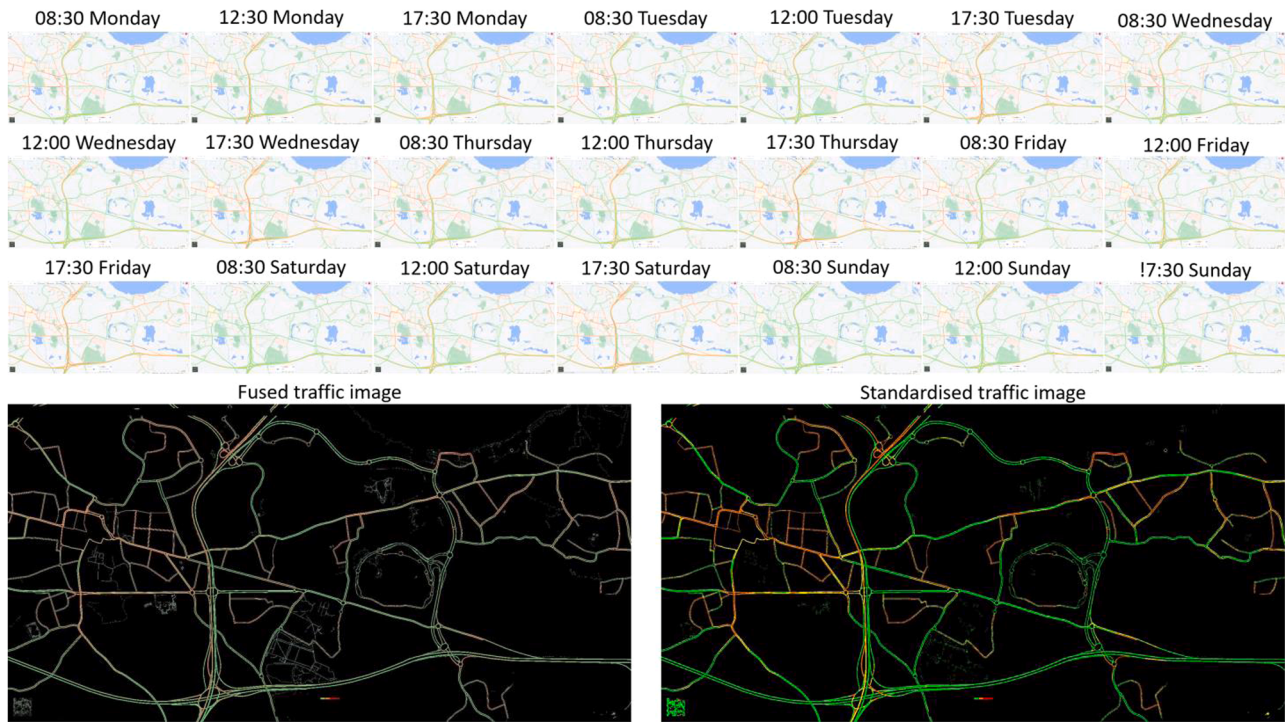


Fig. 19. Traffic congestion images.

Table 6
Parameters for digital image processing.

t_1	t_2	t_3	t_4	t_5
0.234	0.55	1.3	180/255	170/255
t_6	t_7	t_8	t_9	t_{10}
0.234	0.709	1.291	180/255	60/255

2018). According to the data, C_0 in Eqs. (14) for PM_{2.5}, PM₁₀, and NO₂ are set to 15, 27, and 35. According to the method in Section 2.1, the calculation results for the air pollution raster are shown in Fig. 24.

For construction costs, road buffer areas and the vector map of different areas are shown in ① and ② in Fig. 25. The PCM(construction) is given by experts to estimate the costs in the construction cost raster (Table 9). Then the values of cells in different areas can be calculated using Eqs. (15). The result of the construction cost raster is shown in ③

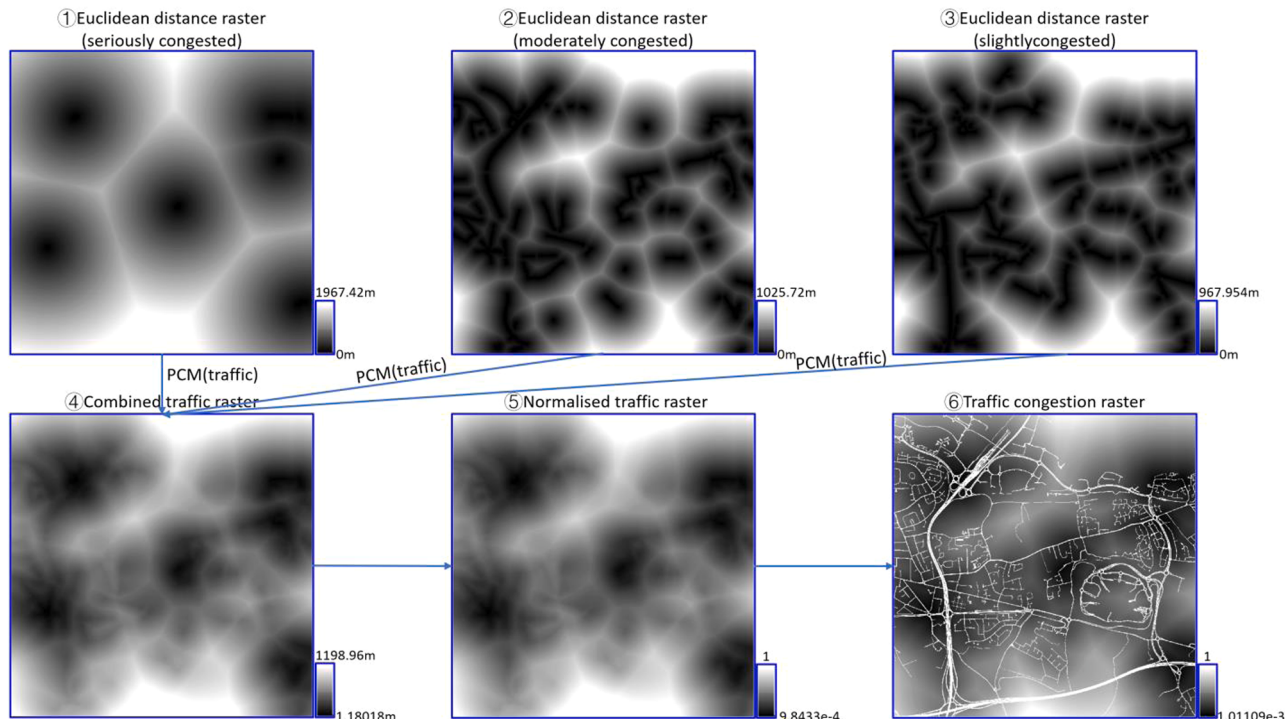
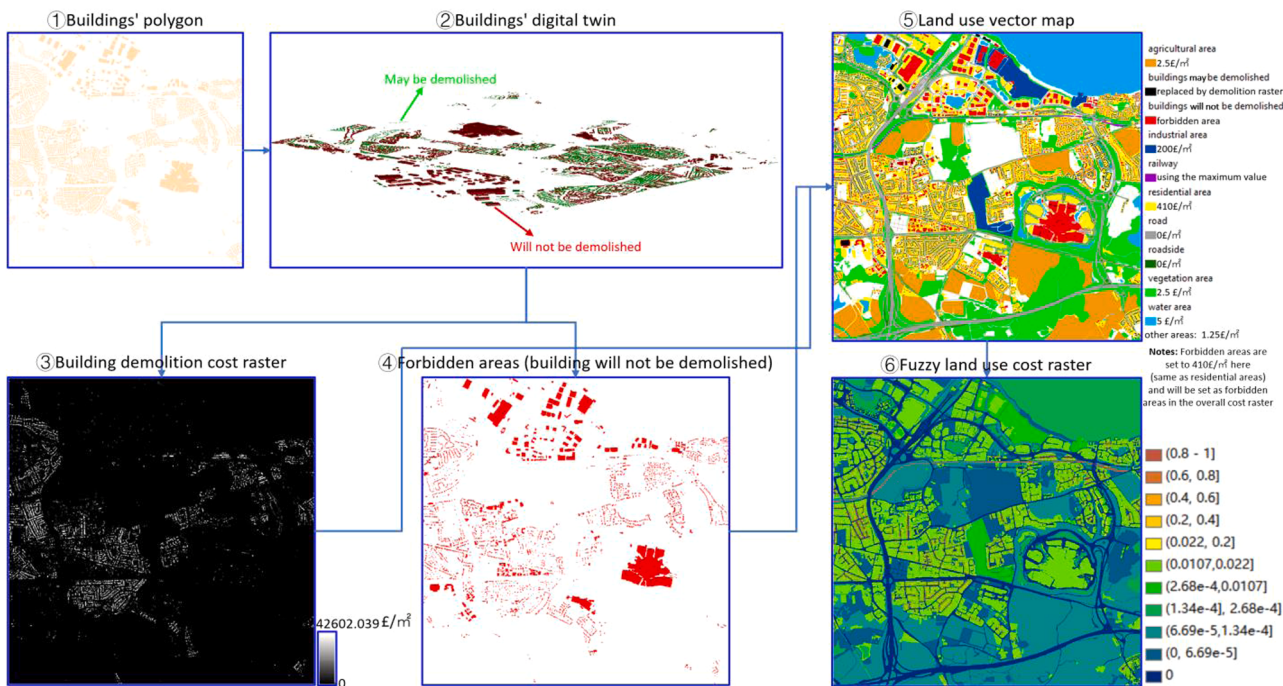
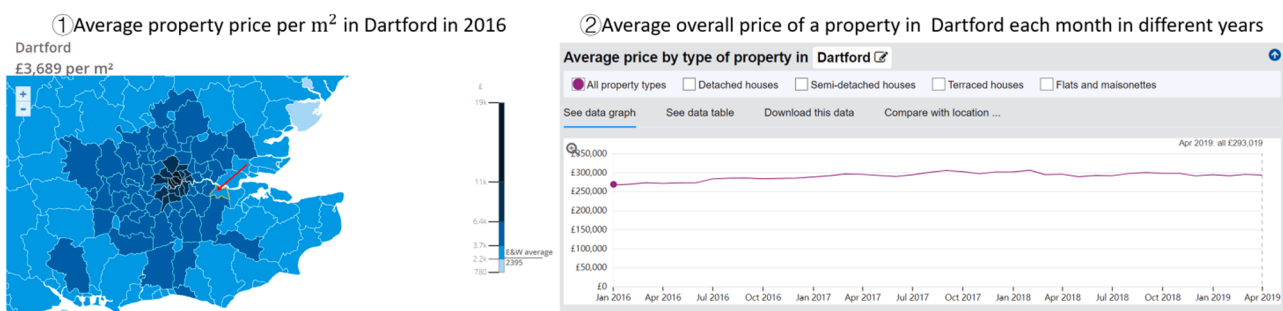


Fig. 20. Traffic congestion rasters.

Table 7

Pairwise comparison matrix for the traffic congestion raster (PCM(traffic)).

PCM(traffic) Different rasters	Euclidean distance raster (seriously congested)	Euclidean distance raster (moderately congested)	Euclidean distance raster (slightly congested)	ω_k in Eq. (10)	Weights ($W(k) = \frac{\omega_k}{\sum_{k=1}^n \omega_k}$)
Euclidean distance raster (Seriously congested)	1	1	2	0.67	0.40
Euclidean distance raster (moderately congested)	1	1	2	0.67	0.40
Euclidean distance raster(slightly congested)	1/2	1/2	1	0.33	0.20

**Fig. 21.** Land use cost raster.**Fig. 22.** Property prices in Dartford.**Table 8**

Property prices in Dartford.

Type Price	Average overall price of a property (P)							
	$P_{January 2016}$	$P_{February 2016}$	$P_{March 2016}$	$P_{April 2016}$	$P_{May 2016}$	$P_{June 2016}$	$P_{July 2016}$	$P_{August 2016}$
Value Type Price Value	266808£	268834£	272788£	270988£	272408£	272664£	282814£	285051£
Average overall price of a property (P)	$P_{September 2016}$	$P_{October 2016}$	$P_{November 2016}$	$P_{December 2016}$	$P_{April 2019}$	P_{2016}	$P_{April 2019}$	$P_{April 2019}$
	285370£	283411£	284318£	284987£	293019£	3689£/m²	3894.79£/m²	

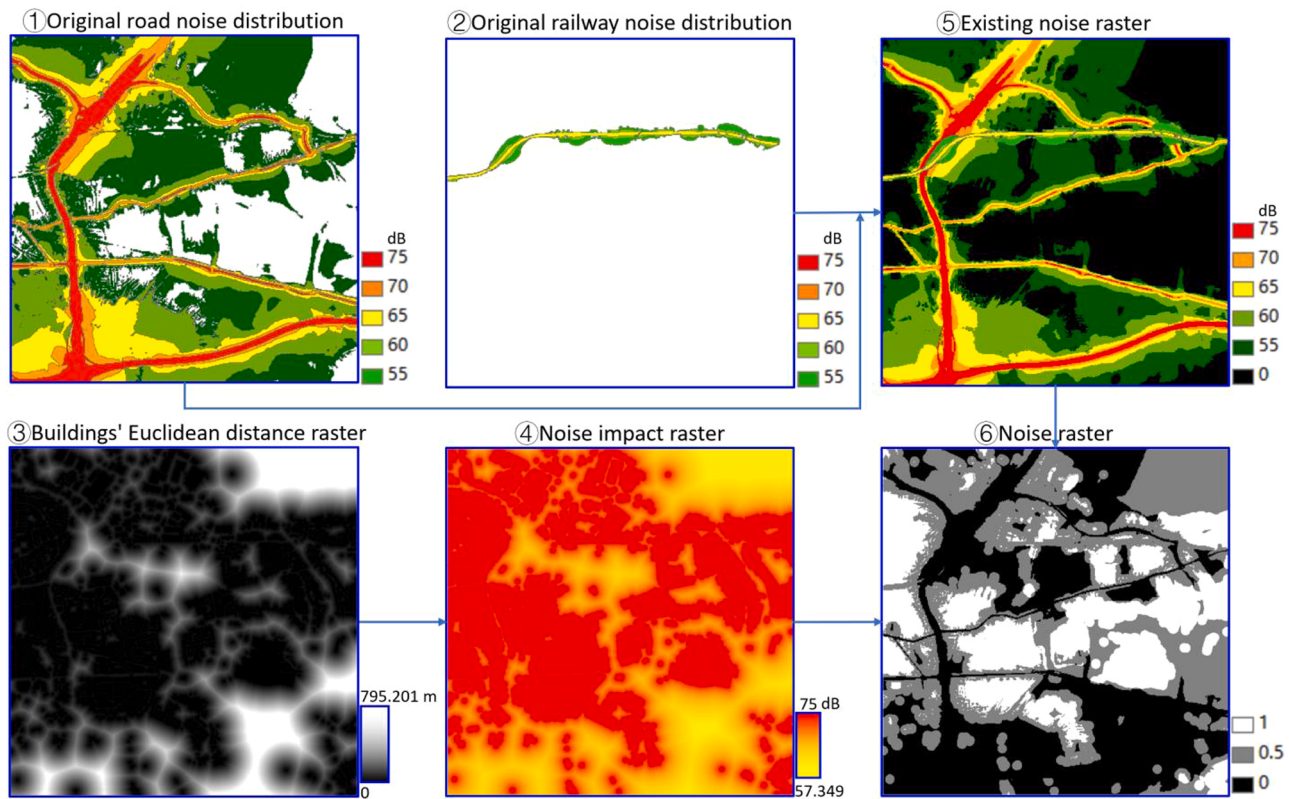


Fig. 23. Original noise distribution data and the calculation results for the noise raster.

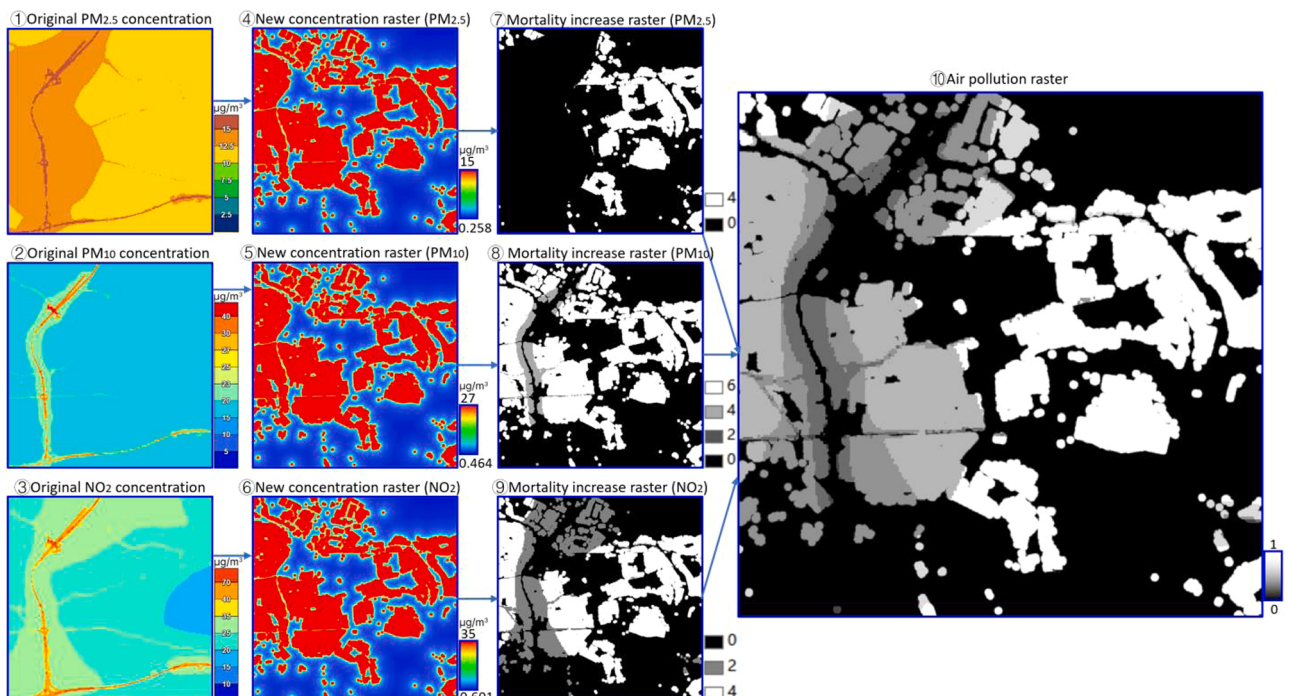


Fig. 24. Original air pollutant concentration data and the calculation results for the air pollution raster.

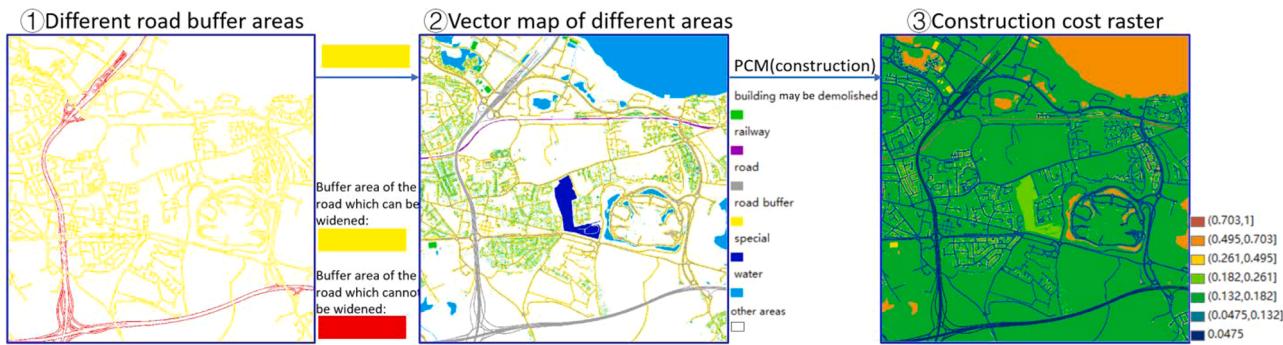


Fig. 25. Construction cost raster.

Table 9

Pairwise comparison matrix for the construction cost raster (PCM(construction)).

PCM(construction)	Railways	Water areas	Buildings may be demolished	Special areas	Other areas	Road buffer areas (roads can be widened)	Roads	ω_k in Eq. (10)	$Cell_k(i,j) = \frac{\omega_k}{\max(\omega_k)}$
Different areas									
Railways	1	2	3	5	6	7	9	0.734	1
Water areas	1/2	1	2	4	5	6	9	0.515	0.702
Buildings may be demolished	1/3	1/2	1	3	4	5	9	0.363	0.494
Special areas	1/5	1/4	1/3	1	2	3	9	0.191	0.260
Other areas	1/6	1/5	1/4	1/2	1	2	8	0.133	0.182
Road buffer areas (roads can be widened)	1/7	1/6	1/5	1/3	1/2	1	7	0.0962	0.131
Roads	1/9	1/9	1/9	1/9	1/8	1/7	1	0.0348	0.0475

Table 10

Pairwise comparison matrix for the cost raster considering 3 factors (PCM(3 factors)).

PCM(3 factors)	Traffic congestion raster	Fuzzy land use cost raster	Construction cost raster	ω_k in Eq. (10)	Weights ($W(k) = \frac{\omega_k}{\sum_{k=1}^n \omega_k}$)
Different rasters					
Traffic congestion raster	1	1/2	1/2	0.333	0.20
Fuzzy land use cost raster	2	1	1	0.667	0.40
Construction cost raster	2	1	1	0.667	0.40

In Fig. 25. In this step, road buffer areas (roads cannot be widened) are regarded as other areas, and their value will be set to 1 in the overall cost map.

3.3. Overall cost raster and road alignment planning

After that, the PCM(3 factors) (Table 10) and PCM(overall)

(Table 11) given by experts are employed to give weights to various rasters to establish the semi-finished cost raster considering 3 factors (⑥ in Fig. 26) (considering traffic congestion, building demolition and land use, and construction cost) and semi-finished overall cost raster (⑦ in Fig. 26) (3 factors, noise, and air pollution). After that, based on the traffic congestion raster (① in Fig. 26), fuzzy land use cost raster (② in Fig. 26), construction cost raster (⑤ in Fig. 26), semi-finished cost raster

Table 11

Pairwise comparison matrix for the overall cost raster (PCM(overall)).

Different rasters	Traffic congestion raster	Fuzzy land use cost raster	Noise raster	Air pollution raster	Construction cost raster	ω_k in Eq. (10)	Weights ($W(k) = \frac{\omega_k}{\sum_{k=1}^n \omega_k}$)
Traffic congestion raster	1	1/2	1/2	1/2	1/2	0.243	0.111
Fuzzy land use cost raster	2	1	1	1	1	0.485	0.222
Noise raster	2	1	1	1	1	0.485	0.222
Air pollution raster	2	1	1	1	1	0.485	0.222
Construction cost raster	2	1	1	1	1	0.485	0.222

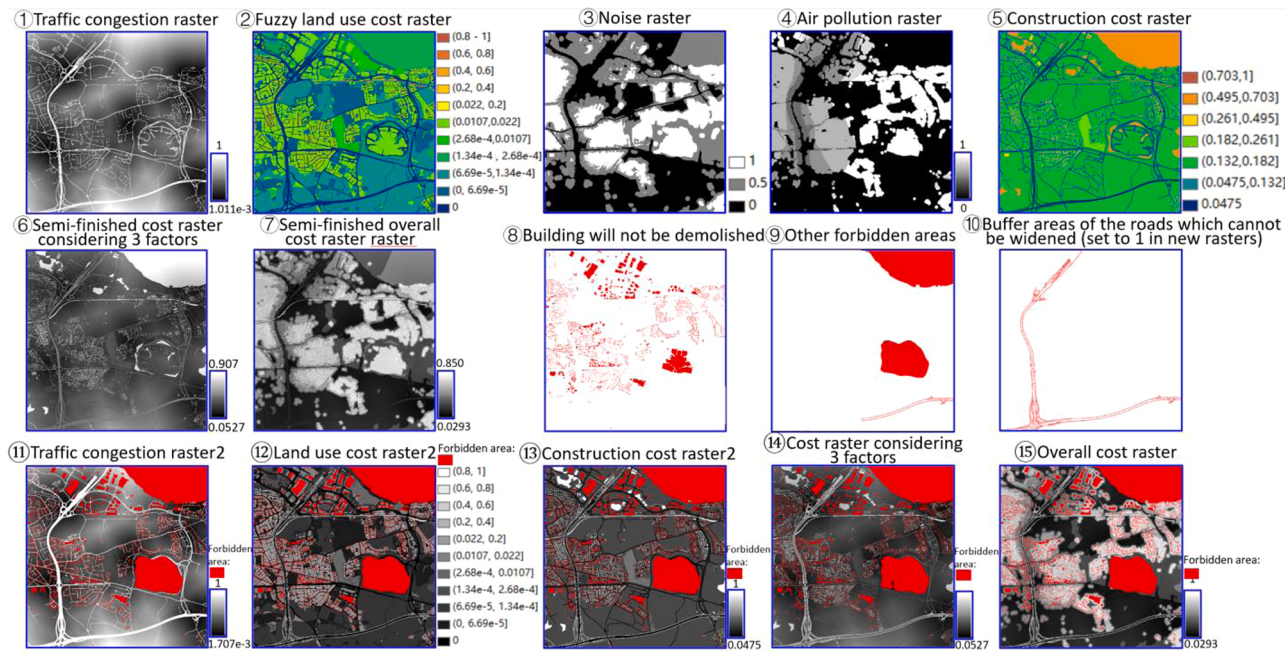


Fig. 26. Overall cost raster.

considering 3 factors (⑥ in Fig. 26), and semi-finished overall cost raster (⑩ in Fig. 26), the value on the buffer areas of the road which cannot be widened (⑪ in Fig. 26), is set to 1. In addition, forbidden areas caused by the buildings that will not be demolished (⑫ in Fig. 26) and other forbidding areas such as River Thames and shopping centres (⑬ in Fig. 26) are set as the final forbidden areas. Then, traffic congestion raster 2 (⑭ in Fig. 26), land use cost raster 2 (⑮ in Fig. 26), construction cost raster 2 (⑯ in Fig. 26), cost raster considering 3 factors (⑰ in Fig. 26), and overall cost raster (⑱ in Fig. 26) can be obtained, respectively. In the raster calculation process, the cell size of the rasters is 0.1m. The cell size of the final cost raster for road alignment planning is set to 2m.

Two-way four-lane roads and two-way eight-lane roads are planned in the case study. According to the UK highway design standard, the width of the two-way four-lane road can be set to 34.1m ((4m side slope and berm+1.5m verge+2.75m hard shoulder+3.65m lane+3.65m lane+0.7 hard strip)*2+1.6 central reserve), and the width of the two-way eight-lane can be set to 49.4m ((4m side slope and berm+1.5m verge+2.75m hard shoulder+3.65m lane+3.7m lane+3.7m lane+3.65m lane+0.7 hard strip)*2+2.1 central reserve), as shown in ① in Fig. 10 (Highways England, 2021). Since the cell size of the final rasters for road alignment planning is 2m, the side length of the brush head drawing a two-way four-lane road occupies 17 cells, and the four-way four-lane road occupies 25 cells. The road alignment planning is conducted on the five rasters (⑪-⑯ in Fig. 26), respectively. Therefore, the road alignment planning with two widths on five cost rasters will have ten results. The zero costs on the land use raster 2 are modified into 1e-9 to limit the length in the zero cost areas.

4. Results and discussion

There are ten alignment planning results, as shown in Figs. 27 and 28. All the alignments do not touch the forbidden areas and try to avoid widening A282 and A2 highways. For alignments considering traffic congestion (① and ② in Fig. 27 and Fig. 28), they try to go through the areas less distant from congested areas. There are some newly built sections and road widening sections. In the road widening section, the road is always on one side and tries to avoid occupying existing old roads because the sections occupying old roads represent the section

without road widening or new road construction, which cannot help ease traffic congestion. For alignments considering land use costs (③ and ④ in Figs. 27 and 28), the alignments try to go through the areas with the lowest land use cost to reduce the overall cost and even detour long distances. The 34m-wide alignment (③ Figs. 27 and 28) takes a long detour to pass through low-cost areas (dark areas) among buildings. However, the spaces between buildings are insufficient to construct a 50m-wide road. Thus, the 50m-wide road (④ in Figs. 27 and 28) chooses another path, and goes over the A2 highway by leveraging an existing bridge of a small road. For alignments considering construction costs (⑤ and ⑥ in Figs. 27 and 28), the alignments try to take advantage of existing main roads as much as possible, even if they cannot alleviate the traffic congestion well. Most sections of the planned road are road widening sections on both sides. The alignments considering three factors (⑦ and ⑧ in Figs. 27 and 28), are the compromise alignments among other alignments considering three factors, respectively. There are some newly built sections and road widening sections. Compared with the corresponding 34m-wide alignments, 50m-wide alignments have significant local changes to avoid high-cost and forbidden areas. In some areas, there is enough space for 34m-wide road construction but not enough for 50m-wide road construction. In addition to the three factors, the alignments considering all factors (⑨ and ⑩ in Figs. 27 and 28) also consider noise impact and air pollution impact. Compared with alignments only considering three factors, they not only try to avoid building demolition, but also try to avoid passing through the existing buildings in the residential areas and keep distance from the existing buildings to alleviate the noise and air pollution impacts on the buildings, even if the land use and construction cost increase locally. The alignments considering all factors can balance the traffic demands, construction cost, and impacts on citizens (building demolition, noise, and air pollution).

Compared with road planning in the natural environment in rural areas, it is challenging to become sustainable for road planning in the built environment in cities due to the limited space. Most existing road alignment planning algorithms do not consider road width and road widening. The case study shows that many existing buildings, road networks, different functional areas, and noise and air pollution impacts can greatly influence road alignment planning in the built environment. When a road is wider, it may touch more areas with different costs and

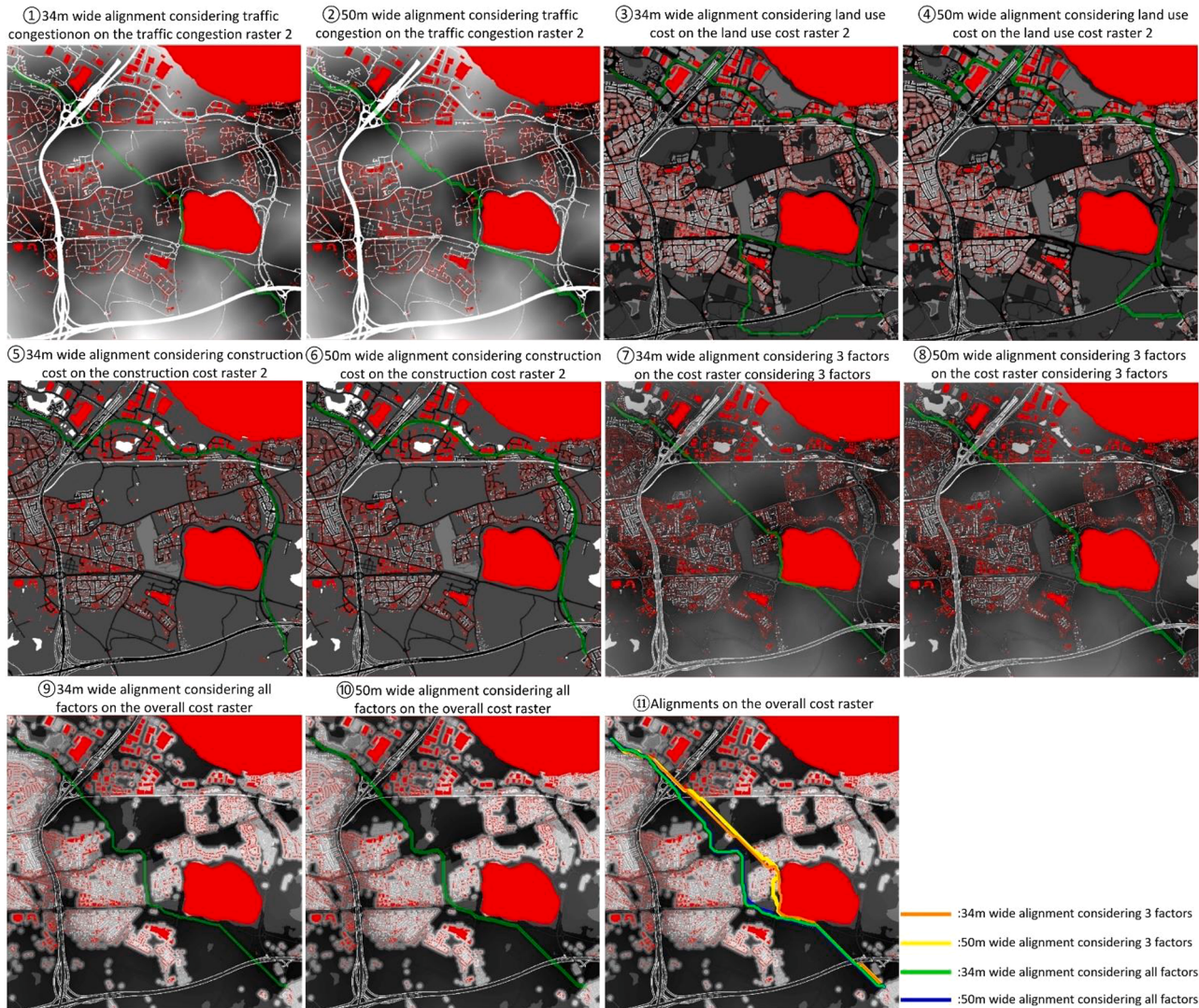


Fig. 27. Results of road alignments on the cost rasters.

even forbidden areas. Thus, an optimal alignment for a road of one width is not necessarily optimal for a road of another width. Roads with different widths will generate various alignment schemes considering various sustainable factors. In addition, there are denser road networks in the cities' built environment compared with rural areas. Road widening can take advantage of existing roads to alleviate traffic congestion with lower construction costs and less impact on other areas. This research is the first to enrich and employ the least-cost wide path algorithm for sustainable road alignment planning in the cities' built environment considering road width and road widening. The alignment planning in the case study can generate several schemes with various road widths, including newly built road sections and road widening sections considering building demolition and land use, traffic congestion, noise impact, air pollution impact, and construction costs.

In addition to the road alignment planning algorithm, how to build digital space (cost raster) to assist in alignment planning is also important. The process is not a simple digitalising process for the built environment in cities from heterogeneous data. It also needs to parse various factors into understandable expressions for road alignment planning. For example, this research proposes several methods to parse the data into different cost rasters considering various sustainable factors. In addition, the definition of forbidden areas and the road buffer areas for road widening also should be considered. The combination of cost

rasters considering various factors from the city should employ MCDM methods, such as AHP in this research, to generate a sustainable and comprehensively optimal solution.

However, there are some limitations in this research. First, more economic, engineering, transportation, social, and environmental factors should be considered. Various corresponding methods need to be proposed to parse various factors into appropriate and understandable expressions for alignment planning. Second, more quantitative and qualitative methods should be employed to evaluate the alignment planning and cost raster creation methods. In addition to quantitative evaluation, focus groups and interviews with more experts based on the design science research (DSR) paradigm are recommended.

5. Conclusion

In the built environment, limited spaces, building demolition, land use, noise and air pollution impacts on residents, and construction costs hinder the achievement of traffic-related goals and sustainable development of the urban road network. The widths of roads can greatly influence road alignment planning in the cities' built environment, and road widening should also be considered, which can take advantage of the existing road to alleviate traffic congestion with lower construction costs and fewer impacts on other areas. Based on the MCDM-GIS

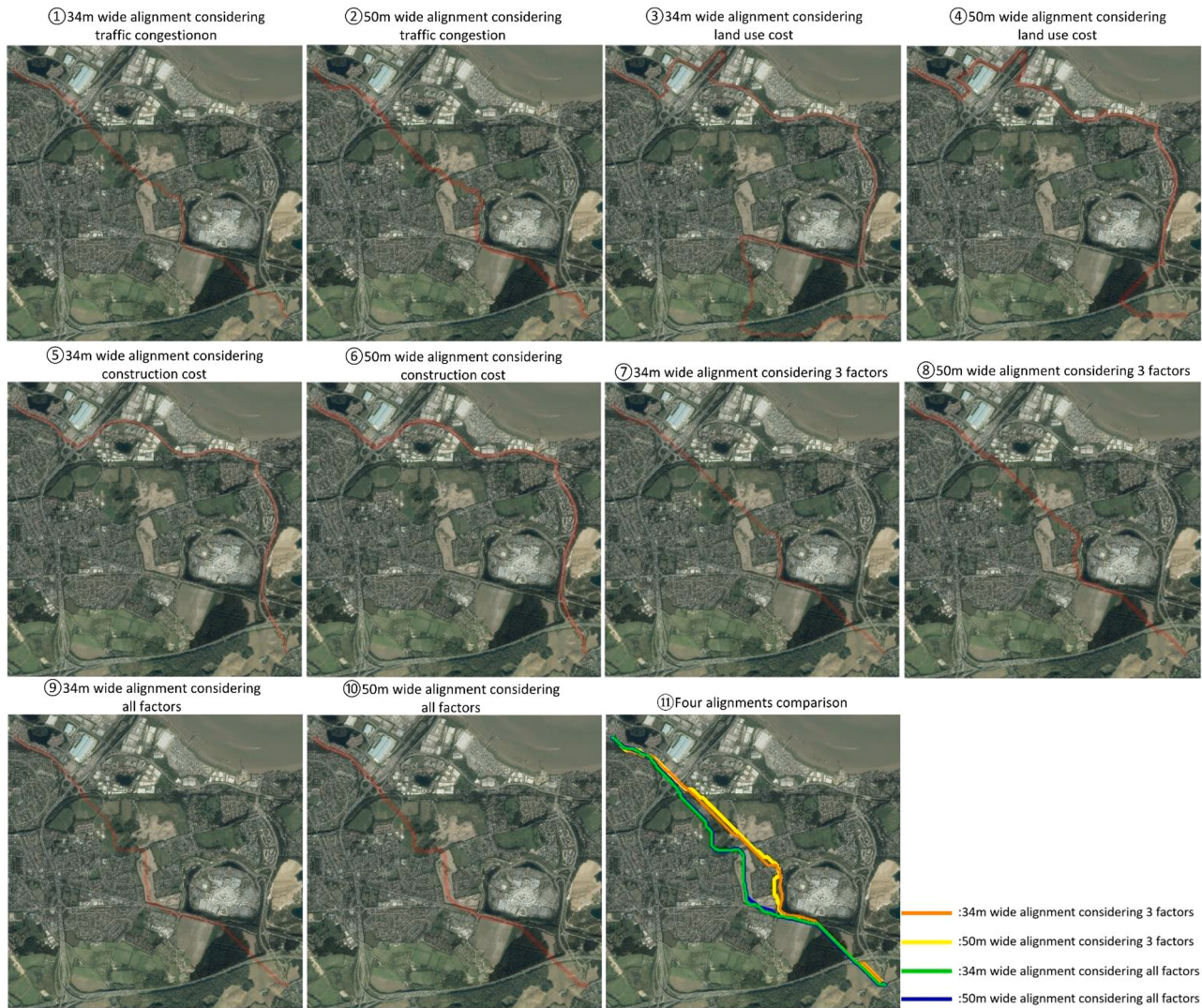


Fig. 28. Results of road alignments on the aerial photograph.

method, this research enriches and employs the least-cost wide path algorithm to plan road alignment in the built environment, considering several sustainable factors, road widths, and road widening. Several methods are proposed to parse various factors into understandable expressions (cost rasters), including building demolition and land use, traffic congestion, noise impact, air pollution impact, and construction costs, to assist in alignment planning. Different cost rasters and road widths can generate different road alignment schemes.

In future research, more engineering, economic, transportation, social, and environmental factors should be considered for road alignment planning in the built environment. In addition to road alignment planning, public transport will be focused on. Furthermore, quantitative methods and qualitative methods such as focus groups and interviews with experts will be conducted based on the design science research (DSR) paradigm to evaluate various sustainable factors, the proposed alignment planning method, and road alignment schemes.

Declaration of Competing Interest

The authors declare that they have no known competing financial interests or personal relationships that could have appeared to influence the work reported in this paper.

Data Availability

Data will be made available on request.

Acknowledgement

This study is supported by Major Science & Technology Project of Hubei (Grant No. 2020ACA006)

Reference

- Addanki, S. C., & Venkataraman, H. (2017). Greening the economy: A review of urban sustainability measures for developing new cities. *Sustainable Cities and Society*, 32, 1–8. <https://doi.org/10.1016/j.scs.2017.03.009>
- Aguiar, M. O., da Silva, G. F., Mauri, G. R., de Mendonca, A. R., Santana, C. J. D., Marcatti, G. E., da Silva, M. L. M., da Silva, E. F., Figueiredo, E. O., Silva, J. P. M., Silva, R. F., Santos, J. S., Lavagnoli, G. L., & Leite, C. C. C. (2021). Optimizing forest road planning in a sustainable forest management area in the Brazilian Amazon. *Journal of Environmental Management*, 288, 11. <https://doi.org/10.1016/j.jenvman.2021.112332>
- Angulo, E., Castillo, E., Garcia-Rodenas, R., & Sanchez-Vizcaino, J. (2012). Determining highway corridors. *Journal of Transportation Engineering*, 138(5), 557–570. [https://doi.org/10.1061/\(asce\)te.1943-5436.0000361](https://doi.org/10.1061/(asce)te.1943-5436.0000361)
- Bindajam, A. A., & Mallick, J. (2020). Impact of the spatial configuration of streets networks on urban growth: A case study of Abha City, Saudi Arabia. *Sustainability*, 12(5), 1–14. <https://doi.org/10.3390/su12051856>

- Cambridge Environmental Research Consultants, *Urban air quality*, (2018)., Retrieved from <https://cerc.co.uk/environmental-research/urban-air-quality.html> (Accessed date: 4 August 2022).
- Cimorelli, A. J., Perry, S. G., Venkatram, A., Weil, J. C., Paine, R. J., Wilson, R. B., Lee, R. F., Peters, W. D., & Brode, R. W. (2005). AERMOD: A dispersion model for industrial source applications. Part I: General model formulation and boundary layer characterization. *Journal of Applied Meteorology*, 44(5), 682–693. <https://doi.org/10.1175/JAM2227.1>
- Davis, C., & Jha, M. K. (2011). A dynamic modeling approach to investigate impacts to protected and low-income populations in highway planning. *Transportation Research Part a-Policy and Practice*, 45(7), 598–610. <https://doi.org/10.1016/j.tra.2011.03.011>
- Department for Communities and Local Government. (2021). *Compulsory purchase and compensation booklet 4: Compensation to residential owners and occupiers*. Retrieved from https://assets.publishing.service.gov.uk/government/uploads/system/uploads/attachment_data/file/571453/booklet4.pdf (Accessed date: 4 August 2022).
- Department for Environment, Food & Rural Affairs. (2019). *Strategic noise mapping (2017)*. Retrieved from <https://www.gov.uk/government/publications/strategic-noise-mapping-2019> (Accessed date: 4 August 2022).
- Dijkstra, E. W. (1959). A note on two problems in connexion with graphs. *Numerische Mathematik*, 1(1), 269–271. <https://doi.org/10.1007/BF01386390>
- Dobrilović, D., Brtka, V., Jotanović, G., Stojanov, Ž., Jauševac, G., & Malić, M. (2022). The urban traffic noise monitoring system based on LoRaWAN technology. *Wireless Networks*, 28(1), 441–458. <https://doi.org/10.1016/10.1007/s11276-021-02586-2>
- Douglas, D. H. (1994). Least-cost path in GIS using an accumulated cost surface and slope lines. *Cartographica*, 31(3), 37–51. <https://doi.org/10.3138/D327-0323-2JUT-016M>
- El Fazziki, A., Benslimane, D., Sadiq, A., Ouarzazi, J., & Sadgal, M. (2017). An agent based traffic regulation system for the roadside air quality control. *IEEE Access*, 5, 13192–13201. <https://doi.org/10.1101/10.1109/ACCESS.2017.2725984>
- Font, A., Baker, T., Mudway, I. S., Purdie, E., Dunster, C., & Fuller, G. W. (2014). Degradation in urban air quality from construction activity and increased traffic arising from a road widening scheme. *Science of the Total Environment*, 497–498, 123–132. <https://doi.org/10.1016/j.scitotenv.2014.07.060>
- Fowler, R. J., & Little, J. J. (1979). Automatic extraction of irregular network digital terrain models. In *Proceedings of Annual Conference on Computer Graphics and Interactive Techniques (SIGGRAPH '79)*, 6th, Vol. 13, Chicago, IL, USA (pp. 199–207). <https://doi.org/10.1145/965103.807444>
- Garcia-Chan, N., Alvarez-Vazquez, L. J., Martinez, A., & Vazquez-Mendez, M. E. (2021). Designing an ecologically optimized road corridor surrounding restricted urban areas: A mathematical methodology. *Mathematics and Computers in Simulation*, 190, 745–759. <https://doi.org/10.1016/j.matcom.2021.06.016>
- Gössling, S. (2020). Why cities need to take road space from cars - and how this could be done. *Journal of Urban Design*, 25(4), 443–448. <https://doi.org/10.1080/13574809.2020.1727318>
- Highways England, Design manual for roads and bridges, CD 127 - Cross-sections and headrooms, (2021)., Retrieved from <https://www.standardsforhighways.co.uk/prod/attachments/10442706-b592-42c8-85f8-2a0c779a8e37?inline=true> (Accessed date: 4 August 2022).
- HM Land Registry Open Data, *UK house price index*, (2021)., Retrieved from <https://landregistry.data.gov.uk/app/ukhpi/browse?from=2016-01-01&location=http%3A%2F%2Flandregistry.data.gov.uk%2Fid%2Fregion%2Fdartford&to=2019-04-01&lang=en> (Accessed date: 4 August 2022).
- Jiang, F., Ma, L., Broyd, T., Chen, W., & Luo, H. (2022). Building digital twins of existing highways using map data based on engineering expertise. *Automation in Construction*, 134. <https://doi.org/10.1016/j.autcon.2021.104081>
- Jiang, F., Ma, L., Broyd, T., Chen, W. Y., & Luo, H. B. (2022). Digital twin enabled sustainable urban road planning. *Sustainable Cities and Society*, 78, 20. <https://doi.org/10.1016/j.scs.2021.103645>
- Karki, T. K., & Lu, B. (2015). What makes, a big and difficult policy enforcement, possible? A success story from Kathmandu Metropolitan City. *Habitat International*, 49, 386–392. <https://doi.org/10.1016/j.habitint.2015.06.011>
- Khomenko, S., Nieuwenhuijsen, M., Ambròs, A., Wegener, S., & Mueller, N. (2020). Is a liveable city a healthy city? Health impacts of urban and transport planning in Vienna, Austria. *Environmental Research*, 183. <https://doi.org/10.1016/j.enres.2020.109238>
- Lazda, Z., & Smirnovs, J. (2011). Research on traffic flow speed of arterial streets in urban areas. In K. D. Froehner, & D. Cygas (Eds.), *8th international conference on environmental engineering, ICEE 2011* (pp. 936–941). Vilnius Gediminas Technical University Publishing House "Technika". <https://www.proquest.com/docview/1462756547?pq-origsite=gscholar&fromopenview=true>
- Ministry of Housing. (2019). *Land value estimates for policy appraisal*. Communities & Local Government. Retrieved from <https://www.gov.uk/government/publications/land-value-estimates-for-policy-appraisal-2019> (Accessed date: 4 August 2022).
- Mondal, M. S., Garg, R. D., Pandey, V., & Kappas, M. (2021). Route alignment planning for a new highway between two cities using Geoinformatics techniques. *Egyptian Journal of Remote Sensing and Space Sciences*, 24(3), 595–607. <https://doi.org/10.1016/j.ejrs.2021.05.003>
- Muneera, C. P., & Karuppanagounder, K. (2022). Economic strategies to alleviate traffic congestion: Evidences from an indian city. In B. Laishram, & A. Tawalare (Eds.), *172. International conference on advances in civil engineering, ACE 2020* (pp. 671–682). Springer Science and Business Media Deutschland GmbH. https://doi.org/10.1007/978-981-16-4396-5_59
- Office for National Statistics, *House prices: How much does one square metre cost in your area?*, (2017)., Retrieved from <https://www.ons.gov.uk/peoplepopulationandcommunity/housing/articles/housepriceshowmuchdoesonesquaremetrecostinyourarea/2017-10-11> (Accessed date: 4 August 2022).
- Office of National Statistics, *How the population changed in Dartford: Census* (2021)., 2021, Retrieved from <https://www.ons.gov.uk/visualisations/censuspopulationchange/E07000107> (Accessed date: 3 September 2022).
- Pushak, Y., Hare, W., & Lucet, Y. (2016). Multiple-path selection for new highway alignments using discrete algorithms. *European Journal of Operational Research*, 248 (2), 415–427. <https://doi.org/10.1016/j.ejor.2015.07.039>
- Saaty, T. L. (1977). A scaling method for priorities in hierarchical structures. *Journal of Mathematical Psychology*, 15(3), 234–281. [https://doi.org/10.1016/0022-2496\(77\)90033-5](https://doi.org/10.1016/0022-2496(77)90033-5)
- Scoppa, M., Bawazir, K., & Alawadi, K. (2018). Walking the superblocks: Street layout efficiency and the sikkak system in Abu Dhabi. *Sustainable Cities and Society*, 38, 359–369. <https://doi.org/10.1016/j.scs.2018.01.004>
- Sheng, N., Xu, Z., & Li, M. (2015). The performance of CRTN model in a Motorcycle city. *Mathematical Problems in Engineering*, 2015. <https://doi.org/10.1155/2015/369620>
- Shirabe, T. (2016). A method for finding a least-cost wide path in raster space. *International Journal of Geographical Information Science*, 30(8), 1469–1485. <https://doi.org/10.1080/13658816.2015.1124435>
- Singh, M. P., & Singh, P. (2017). Multi-criteria GIS modeling for optimum route alignment planning in outer region of Allahabad City. *India, Arabian Journal of Geosciences*, 10(13), 16. <https://doi.org/10.1007/s12517-017-3076-z>
- Sitzia, T., Rizzi, A., Cattaneo, D., & Semenzato, P. (2014). Designing recreational trails in a forest dune habitat using least-cost path analysis at the resolution of visitor sight distance. *Urban Forestry and Urban Greening*, 13(4), 861–868. <https://doi.org/10.1016/j.ufug.2014.09.011>
- Snyder, M. G., Venkatram, A., Heist, D. K., Perry, S. G., Petersen, W. B., & Isakov, V. V. (2013). RLNE: A line source dispersion model for near-surface releases. *Atmospheric Environment*, 77, 748–756. <https://doi.org/10.1016/j.atmosenv.2013.05.074>
- Vázquez-Méndez, M. E., Casal, G., Castro, A., & Santamarina, D. (2021). An algorithm for random generation of admissible horizontal alignments for optimum layout design. *Computer-Aided Civil and Infrastructure Engineering*, 36(8), 1056–1072. <https://doi.org/10.1111/mice.12682>
- Vazquez-Mendez, M. E., Casal, G., Santamarina, D., & Castro, A. (2018). A 3D model for optimizing infrastructure costs in road design. *Computer-Aided Civil and Infrastructure Engineering*, 33(5), 423–439. <https://doi.org/10.1111/mice.12350>
- Wang, H., Cai, M., & Yao, Y. (2017). A modified 3D algorithm for road traffic noise attenuation calculations in large urban areas. *Journal of Environmental Management*, 196, 614–626. <https://doi.org/10.1016/j.jenvman.2017.03.039>
- World Health Organization, *Environmental health criteria 12: Noise*, (1980)., Retrieved from <https://apps.who.int/iris/bitstream/handle/10665/39458/9241540729-eng.pdf> (Accessed date: 4 August 2022).
- World Health Organization, WHO global air quality guidelines: Particulate matter (PM_{2.5} and PM₁₀), ozone, nitrogen dioxide, sulfur dioxide and carbon monoxide, (2021)., Retrieved from <https://apps.who.int/iris/bitstream/handle/10665/34532/9/9789240034228-eng.pdf> (Accessed date: 4 August 2022).
- Zeng, G. W., Sun, Z. Y., Liu, S. Y., Chen, X. Q., Li, D. Q., Wu, J. J., & Gao, Z. Y. (2021). Percolation-based health management of complex traffic systems. *Frontiers of Engineering Management*, 8(4), 557–571. <https://doi.org/10.1007/s42524-021-0174-0>
- Zhang, Z. Y., Lu, L. J., Zhu, L., Zhang, W. Y., & Yang, J. (2020). Preference information incorporation for decision making in the biobjective alignment optimization problem of river-crossing tunnels. *Journal of Transportation Engineering Part a-Systems*, 146(10), 10. <https://doi.org/10.1061/jtepb.0000443>
- Zhong, Q., & Liu, Q. (2021). Automatic generation of urban road planning network under deep learning. In W. Wei, & J. Han (Eds.), *2074. 2021 international conference on information technology and big data engineering, ITBDE 2021*. IOP Publishing Ltd. <https://doi.org/10.1088/1742-6596/2074/1/012088>.
- Old Oak and Park Royal Development Corporation, *Tall buildings statement*, (2018)., Retrieved from https://www.london.gov.uk/sites/default/files/52_tall_buildings_statement_2018.pdf (Accessed date: 4 August 2022).